

94
8/25/78

LA-7245

16.391

UC-45

Issued: July 1978

MASTER

Burning and Detonation

Charles A. Forest

University of California



LOS ALAMOS SCIENTIFIC LABORATORY

Post Office Box 1663 Los Alamos, New Mexico 87545

DISTRIBUTION OF THIS DOCUMENT IS UNLIMITED

DISCLAIMER

This report was prepared as an account of work sponsored by an agency of the United States Government. Neither the United States Government nor any agency thereof, nor any of their employees, makes any warranty, express or implied, or assumes any legal liability or responsibility for the accuracy, completeness, or usefulness of any information, apparatus, product, or process disclosed, or represents that its use would not infringe privately owned rights. Reference herein to any specific commercial product, process, or service by trade name, trademark, manufacturer, or otherwise does not necessarily constitute or imply its endorsement, recommendation, or favoring by the United States Government or any agency thereof. The views and opinions of authors expressed herein do not necessarily state or reflect those of the United States Government or any agency thereof.

DISCLAIMER

Portions of this document may be illegible in electronic image products. Images are produced from the best available original document.

An Affirmative Action/Equal Opportunity Employer

This report was prepared as an account of work sponsored by the United States Government. Neither the United States nor the United States Department of Energy, nor any of their employees, nor any of their contractors, subcontractors, or their employees, makes any warranty, express or implied, or assumes any legal liability or responsibility for the accuracy, completeness, or usefulness of any information, apparatus, product, or process disclosed, or represents that its use would not infringe privately owned rights.

**UNITED STATES
DEPARTMENT OF ENERGY
CONTRACT W-7405-ENG. 36**

NOTICE

PORTIONS OF THIS REPORT ARE ILLEGIBLE. It
has been redacted from the best available
copy to permit the broadest possible availa-
bility.

BURNING AND DETONATION

by

Charles A. Forest

NOTICE

This report was prepared as an account of work sponsored by the United States Government. Neither the United States nor the United States Department of Energy, nor any of their employees, nor any of their contractors, subcontractors, or their employees, makes any warranty, express or implied, or assumes any legal liability or responsibility for the accuracy, completeness or usefulness of any information, apparatus, product or process disclosed, or represents that its use would not infringe privately owned rights.

ABSTRACT

The effect of a confined porous bed of burning explosive abutting solid explosive is studied by computer simulation. Burning only is allowed in the porous bed; shock-induced decomposition is modeled by FOREST FIRE in the solid material. The occurrence of detonation in the solid explosive depends on the surface-to-volume ratio, the confinement of the porous bed, and the geometry of the system.

The density effect on the initial-shock-pressure, distance-to-detonation (wedge test) measure of shock sensitivity is calculated. The calculation uses the invariance with density of the shock particle velocity as a function of time to detonation.

I. INTRODUCTION

Sometimes a high explosive that is initially burning will detonate. The change from burn to detonation is known as Deflagration-to-Detonation Transition (DDT). Accidents with high explosives may often involve DDT, and for this reason alone, the subject is of interest.

Linear burn of an explosive proceeds at a rate of 10 to 100 cm/s, whereas detonation waves propagate at a rate of 0.3 to 0.9 cm/ μ s. The rates are very different, and special conditions are necessary for the transition to occur. Conditions conducive to the occurrence of DDT are confinement of a region with a large surface area burning and high shock sensitivity of the same or nearby material. The surface area may be initially present or may be dynamically produced as a result of stress on the material. The confinement is provided both by material strength and inertia of the confining material. The presence of a large burning surface area increases the mass burn rate, which, if the confinement is sufficient, leads to high pressures and shock formation. If the shock is strong enough, the explosive begins to decompose, the shock grows, and finally a detonation is produced.

The burning in a porous bed, known as convective combustion, is a complicated matter. In addition to the role of high mass burning rate and confinement, the flow of hot gas relative to the bed of particles is often important especially in a large porous bed. The flow gases enter into the fluid dynamics (a

two-phase flow problem) and transfer heat to the particles. Ignition, flame spreading, and flame structure in the voids are also involved. (Burning of gun propellant involves many of these processes.)

II. A SPECIAL CASE

Rather than try to model such a large collection of processes, a model is constructed here that involves only confined burning and shock initiation. The case considered involves mostly solid explosive, a small region of porous material, and some sort of confinement. (Such situations may relate better to accidents because it seems unlikely that a piece of explosive will turn entirely to dust because it is dropped.) A small region of porous material may be just too small to produce a DDT by itself. However, if the small region abuts a large piece of solid explosive, which provides confinement, detonation may occur in the solid. The burning of the porous material need not proceed at detonation rates but need only burn fast enough to form a shock in the solid. If the solid is sensitive to shock-induced decomposition and the shock is strong enough, the shock will grow into a detonation wave.

To numerically study this restricted case of the DDT, a sequence of problems has been calculated (see Fig. 1) in which the confinement, the burn rate, and the geometry are varied. Three types of confinement are considered: (1) the porous region is between solid explosive and an aluminum case with a rigid back boundary (problem geometry I), (2) the porous region is between solid explosive and an aluminum case that can move into air (problem geometries II, III, and V), (3) the porous region is contained in solid explosive alone (problem geometry IV). Three geometries are included: (1) planar (problem geometries I, II, and V), (2) cylindrical converging (problem geometry III), (3) cylindrical diverging (problem geometry IV). The mass burn in the porous region is simulated by the bulk burn model described in Appendix A. Bulk burn assumes that the porous region is composed of particles of similar geometry with some initial surface-to-volume ratio S_0/V_0 or $(S/V)_0$. For each problem geometry, calculations are made for various initial ratios. The bulk burn rates for $S_0/V_0 = 75/\text{cm}$ and $S_0/V_0 = 100/\text{cm}$ are displayed in Fig. 2. Note here that for a cube with side length of 0.1 cm, $(S/V)_0 = 60/\text{cm}$, and for a cube of 0.01 cm, $(S/V)_0 = 600/\text{cm}$.

Shock-induced decomposition of the solid explosive is simulated with the FOREST FIRE¹ model described in Appendix B. In these problems the decomposition rate is taken to be a function of pressure only. The FOREST FIRE rates at densities $\rho = 1.91$ and $\rho = 1.72$ as a function of pressure are shown in Fig. 2. The experimental and calculated curves of distance to detonation versus shock pressure for HE-X* that give the basis for the rate calculation are shown in Fig. 3. Table I gives the HOM equation-of-state² constants for aluminum and for HE-X at two densities. Also in Table I are the constants to the fit of the pressure-dependent rate function displayed in Fig. 2. The problems were run with the SIN one-dimensional Lagrangian hydrodynamics code.² The initial cell length in each region is $\Delta X = 0.1 \text{ cm}$.

To illustrate the effect of a low-density (high shock sensitivity) region contained within the solid explosive, one problem is calculated using problem geometry V (Fig. 1). Here, a 1.0-cm slab of $\rho = 1.72$ HE-X is embedded in the solid and reacts by the FOREST FIRE model. The increased rates, calculated by the POP-PLOT extrapolation method described in Appendix B, are shown in Fig. 2.

*An experimental HMX-based explosive.

1-D PLANE

Problem Geometry I

RIGID WALL	ALUMINUM 4 cm	HE-X (1.91) 10 cm FOREST FIRE	HE-X (1.72) 2 cm BULK BURN	ALUMINUM 4 cm	RIGID WALL
---------------	------------------	-------------------------------------	----------------------------------	------------------	---------------

Problem Geometry II

AIR 2 cm	ALUMINUM 2 cm	HE-X (1.91) 10 cm FOREST FIRE	HE-X (1.72) 2 cm BULK BURN	ALUMINUM 2 cm	AIR 2 cm
-------------	------------------	-------------------------------------	----------------------------------	------------------	-------------

1-D CYLINDER

Problem Geometry III

CENTER •	HE-X (1.91) 10 cm FOREST FIRE	HE-X (1.72) 2 cm BULK BURN	ALUMINUM 2 cm	AIR 2 cm
-------------	-------------------------------------	----------------------------------	------------------	-------------

Problem Geometry IV

CENTER •	HE-X (1.72) 2 cm BULK BURN	HE-X (1.91) 10 cm FOREST FIRE	ALUMINUM 2 cm	AIR 2 cm
-------------	----------------------------------	-------------------------------------	------------------	-------------

1-D PLANE

Problem Geometry V

AIR 2 cm	ALUMINUM 2 cm	HE-X (1.91) 5.5 cm FOREST FIRE	HE-X (1.72) 1.0 cm FOREST FIRE	HE-X (1.91) 3.5 cm FOREST FIRE	HE-X (1.72) 2 cm FOREST FIRE	ALUMINUM 2 cm	AIR 2 cm
-------------	------------------	--------------------------------------	--------------------------------------	--------------------------------------	------------------------------------	------------------	-------------

Fig. 1.
Problem geometries for HE-X burning and detonation.

III. DISCUSSION

Calculations with the SIN hydrodynamics code are shown in Figs. 4a through 4l. In each frame of the figures is shown a graph of pressure as a function of distance and a graph of mass fraction as a function of distance. The pressure scale is given in the lower right corner (for example, 50 kbar). The mass fraction scale is always 0. to 1.0. Time indicated on each frame is in microseconds. The initial S/V for the bulk burn region is as specified for each figure.

Comparison of the problems gives some insight into the importance of the various boundary conditions, geometric symmetry, and processes. Consider first the sequence of planar problems using problem geometries I and II. In these problems the effect of the two boundary conditions on the aluminum depends on $(S/V)_0$. If $(S/V)_0 = 400$ cm (Figs. 4a and 4b), the bulk burn is so fast that the aluminum back boundary makes no difference. With $(S/V)_0 = 100/\text{cm}$ (Figs. 4c and 4d), the effect of the boundary begins to show somewhat in the small increase in time to detonation and in the pressure wave. With $(S/V)_0 = 75/\text{cm}$ (Figs. 4e and 4f), the difference is considerable—detonation at 39.83 μs with problem geometry I and no detonation with problem geometry II. In II, the problem is terminated just as the pressure wave is starting to reflect off the left piece of aluminum. If run further, the reflected wave would cause detonation in the model because FOREST FIRE as used here is pressure dependent. However, if the first wave desensitizes the HE-X, detonation may not occur. The matter is open for further study.

Next consider the cylindrical converging problems (problem geometry III) with $(S/V)_0 = 100/\text{cm}$ and $(S/V)_0 = 75/\text{cm}$ (Figs. 4g and 4h). These are similar to the planar problem geometry II problems, but detonation occurs for both ratios; cylindrical convergence of the wave is the contributing factor.

The sequence of problems with problem geometry IV (Figs. 4i through 4k) illustrates the balance between the bulk burn and the diverging wave that lowers the pressure. The problem of $(S/V)_0 = 130/\text{cm}$ detonates just before the wave reaches the outer case, whereas $(S/V)_0 = 100/\text{cm}$ fails to detonate. Comparison of these diverging problems with the planar and cylindrical converging problems shows that geometry is a very significant factor in the outcome.

Problem geometry V is similar to problem geometry II except for the inclusion of a 1.0-cm region of lower density HE-X. The problem with $(S/V)_0 = 75/\text{cm}$ (Fig. 4l) shows detonation occurs about 1.4 cm into the $\rho = 1.91$ HE-X past the lower density region. The presence of the low-density region noticeably alters the pressure wave, even though detonation did not occur in the $\rho = 1.72$ HE-X region. The pressure wave as incident on the $\rho = 1.72$ HE-X region is too low to cause detonation to occur in a 1.0-cm run, however it is sufficient to induce significant partial decomposition, which adds to the wave causing detonation in the adjacent high-density HE-X.

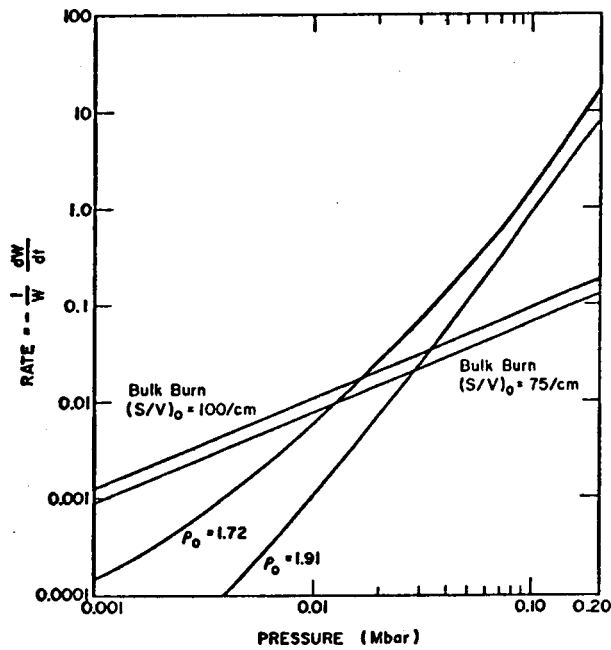


Fig. 2.
FOREST FIRE shock decomposition rates
for HE-X at two densities and two bulk
burn rates for HE-X at $\rho = 1.72$.

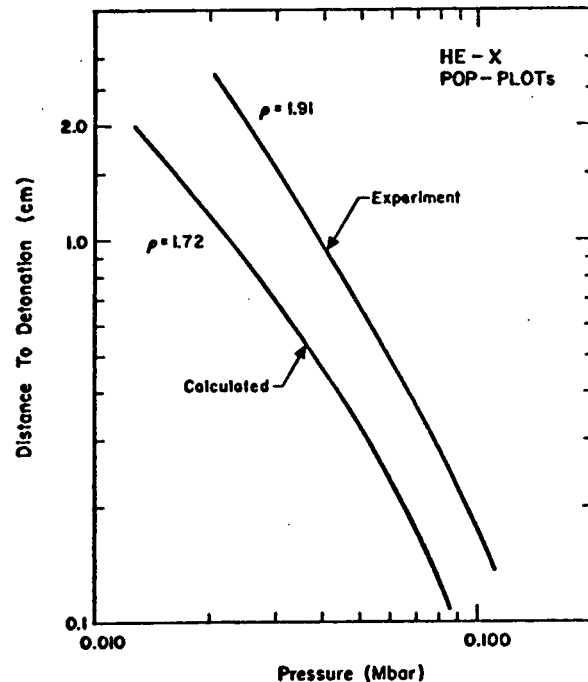


Fig. 3.
Distance to detonation vs initial shock
pressure for HE-X.

TABLE I

HOM EQUATION-OF-STATE CONSTANTS FOR ALUMINUM AND
 HE-X ($\rho = 1.91$ AND $\rho = 1.72$ g/cm³) AND THE POLYNOMIAL COEFFICIENTS
 FOR THE PRESSURE-DEPENDENT FOREST FIRE RATE

ALUMINUM, RHO = 2,785				
HOM CONSTANTS FOR A SOLID				
5,3500000000E-01	1,3500000000E+00	1,0000000000E-01	0,	
0,	-7,96115866474E+01	-3,17533561633E+02	-4,36525371533E+02	
-2,64248248960E+02	-5,79734964732E+01	1,7000000000E+00	2,2000000000E+01	
3,5946427289E+01	2,4000000000E-05	0,	1,152400000000E+00	
3,0200000000E+02	1,02000200000E-06	3,6666666666E-03	2,50000000000E+01	
5,0000000000E-02	1,0000000000E-06	0,		

HE-X, RHO=1,91				
HOM CONSTANTS FOR THE SOLID EXPLOSIVE				
2,784450000000E-01	3,620000000000E+00	4,784450000000E-01	2,430000000000E+01	
1,879300000000E+00	-1,35733168580E+01	-8,64978401037E+01	-1,42462911736E+02	
-9,99233449144E+01	-2,35377505339E+01	1,500000000000E+00	3,300000000000E+01	
5,23560209424E-01	1,200000000000E-04	0,	0,	
2,968790000000E+02	0,	0,	0,	
0,	0,	4,784450000000E-01		
HOM CONSTANTS FOR THE DETONATION PRODUCTS				
-3,5927507104E+00	-2,2513995825E+00	3,07083271071E-01	-3,38388105816E+02	
3,26317134386E-04	-1,5695759961E+00	5,61240444420E-01	9,14476859528E+02	
8,61248912339E-03	3,29348178818E-04	8,05038175417E+00	-4,75298681181E-01	
1,23767476473E-01	5,25836057192E-03	-4,21628859215E-03	5,00000000000E+01	
1,00000000000E-01				
HE-X FIRE, RHO=1.91, DCJ=0.8093				
15 CONSTANTS FOR THE FIRE FIT ON THE PRESSURE INTERVAL .010 TO .450 MBARS, $DW/DT = -w*EXP(C(1)+C(2)*P+...,+C(N)*P^(N-1))$				
-1,03043211330E+01	4,98373275331E+02	-1,75022603100E+04	4,38741848365E+05	
-7,57748147863E+06	8,95573881711E+07	-7,61498375236E+08	4,68779740935E+09	
-2,10524741635E+10	6,88859037514E+10	-1,02268213517E+11	2,67785400124E+11	
-2,93612090928E+11	1,92015352041E+11	-5,66557921595E+10		

HE-X, RHO=1.7190 = 0.9*1.91				
HOM CONSTANTS FOR THE SOLID EXPLOSIVE				
5,8000000000E-02	4,4000000000E+00	4,856930000000E-01	1,273700000000E-01	
2,416000000000E+00	5,35368101554E+01	2,8042429325E+02	6,10873944231E+02	
5,87554896556E+02	2,12269494127E+02	1,500000000000E+00	3,300000000000E+01	
5,81733566027E-01	1,200000000000E-04	0,	0,	
3,030000000000E+02	0,	0,	0,	
0,	0,	4,856930000000E-01		
HOM CONSTANTS FOR THE DETONATION PRODUCTS				
-3,4582964362E+00	-2,21293918558E+00	2,84088396236E-01	-3,45908309471E-02	
1,61341661461E-03	-1,5276950343E+00	5,11751877215E-01	6,91301026740E-02	
5,09642892264E-03	1,40021106127E-04	8,14735025976E+00	-4,29018154047E-01	
8,86488937240E-02	-1,18036109477E+02	6,09785049038E-04	5,000000000000E+01	
1,220000000000E-01				
HE-X, FIRE, RHO=1.7190=0.9*1.91, DCJ = 0.7484				
15 CONSTANTS FOR THE FIRE FIT ON THE PRESSURE INTERVAL .001 TO .010 MBARS, $DW/DT = -w*EXP(C(1)+C(2)*P+...,+C(N)*P^(N-1))$				
-1,03624756544E+01	2,35852256224E+03	-9,58087572371E+05	2,92842146127E+08	
-5,66925456239E+10	7,45365730550E+12	-1,32313095885E+15	3,94621241727E+17	
-8,74470711042E+19	1,16911063069E+22	-9,20901241499E+23	3,97259564780E+25	
-7,26924113139E+26				

15 CONSTANTS FOR THE FIRE FIT ON THE PRESSURE INTERVAL .010 TO .370 MBARS, $DW/DT = -w*EXP(C(1)+C(2)*P+...,+C(N)*P^(N-1))$				
-7,86511750275E+00	3,69724700255E+02	-1,28370406823E+04	3,44910103509E+05	
-6,54018384861E+06	8,81003475630E+07	-8,5677830388E+08	6,89069383860E+09	
-3,18292752849E+10	1,21957586372E+11	-3,38173618326E+11	6,59827939544E+11	
-8,58557307437E+11	6,68425806956E+11	-2,35424504376E+11		

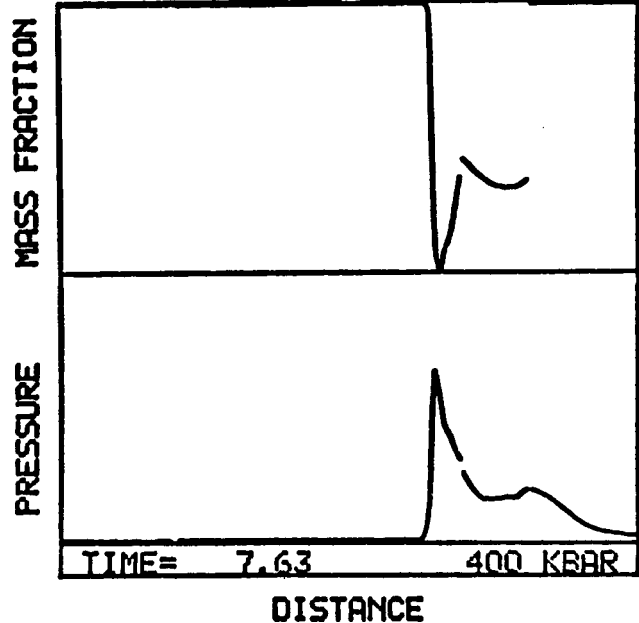
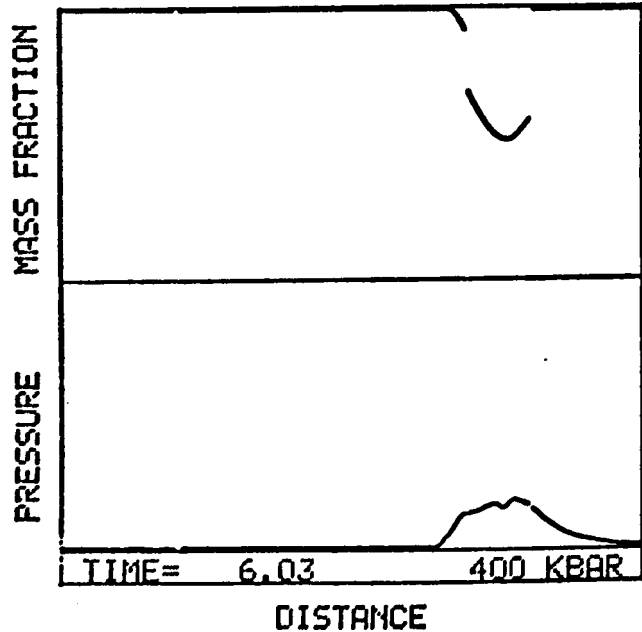
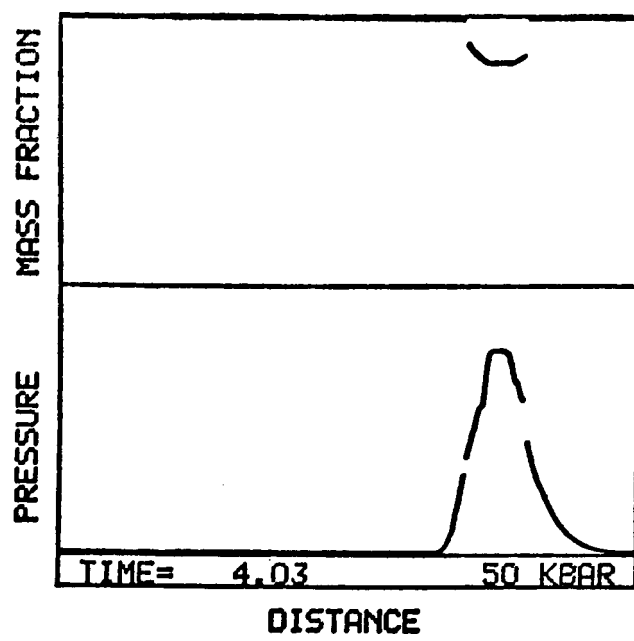
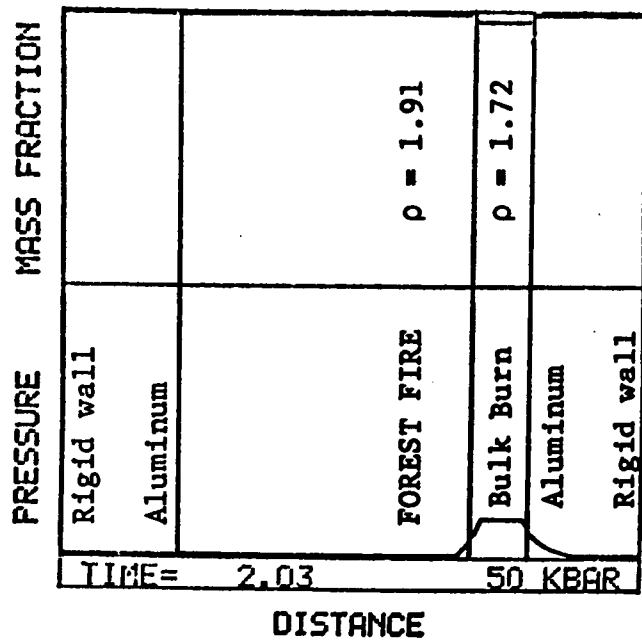


Fig. 4a.

SIN calculation for a 1-D plane in problem geometry I with $(S/V)_0 = 400/\text{cm.}$

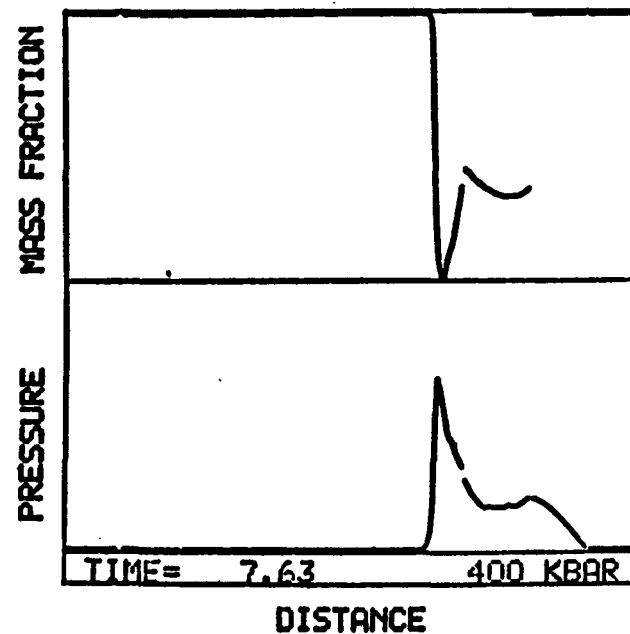
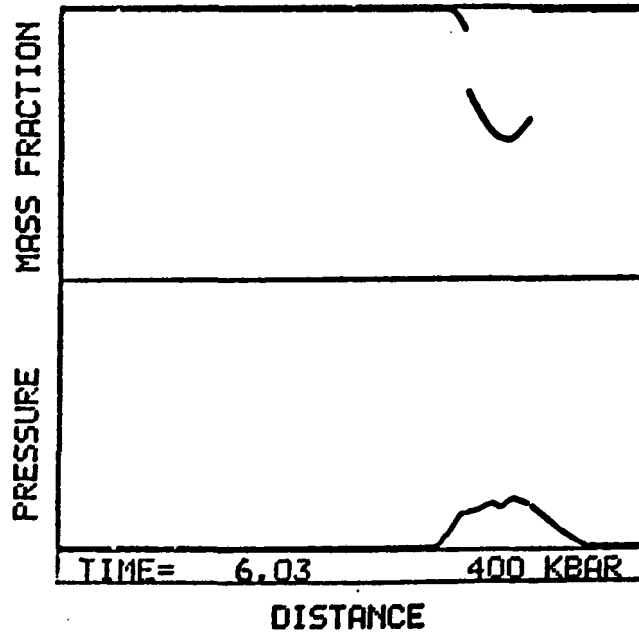
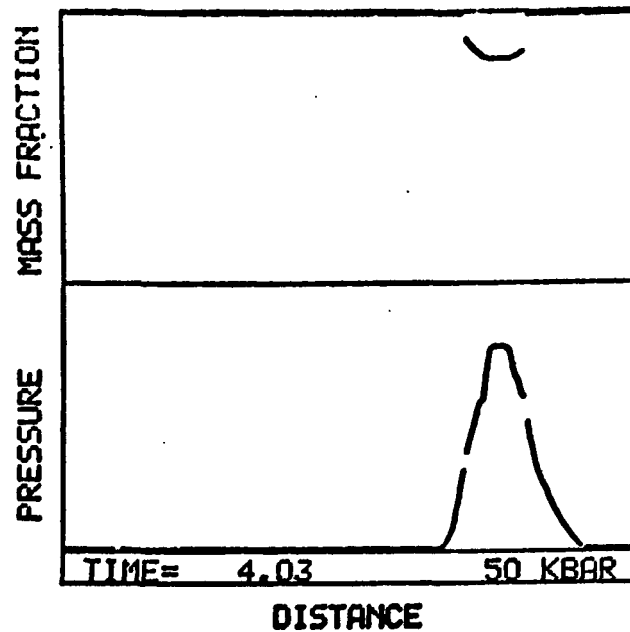
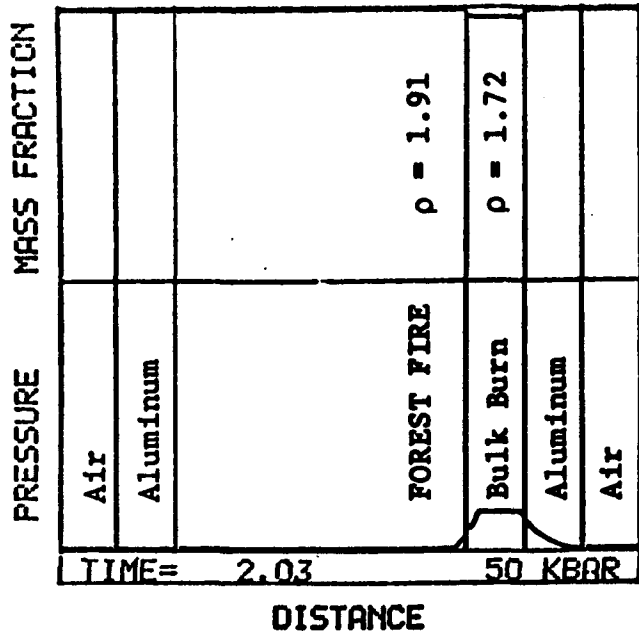


Fig. 4b.
SIN calculation for a 1-D plane in problem geometry II with $(S/V)_0 = 400/\text{cm}.$

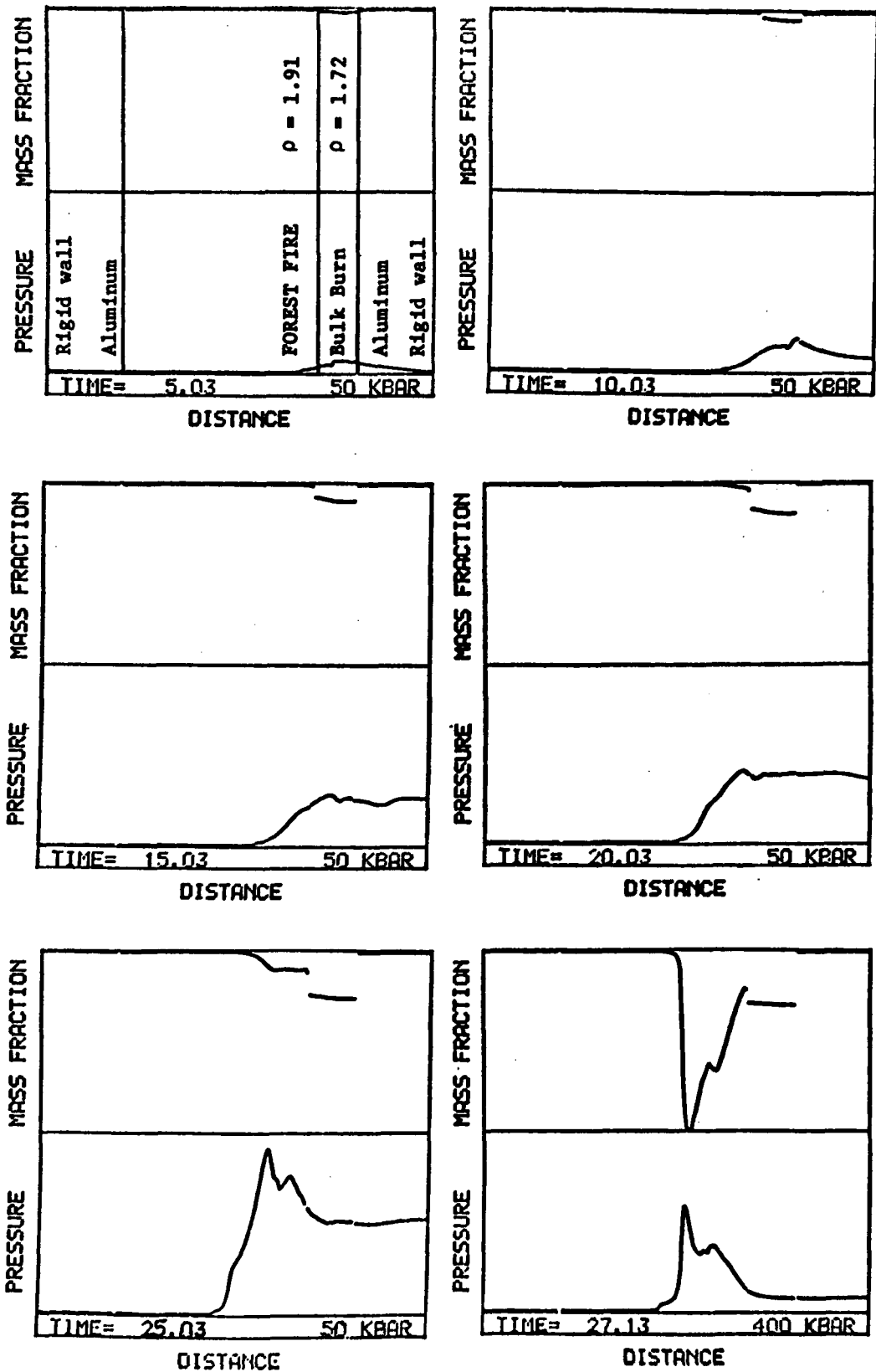


Fig. 4c.

SIN calculation for a 1-D plane in problem geometry I with $(S/V)_0 = 100/\text{cm.}$

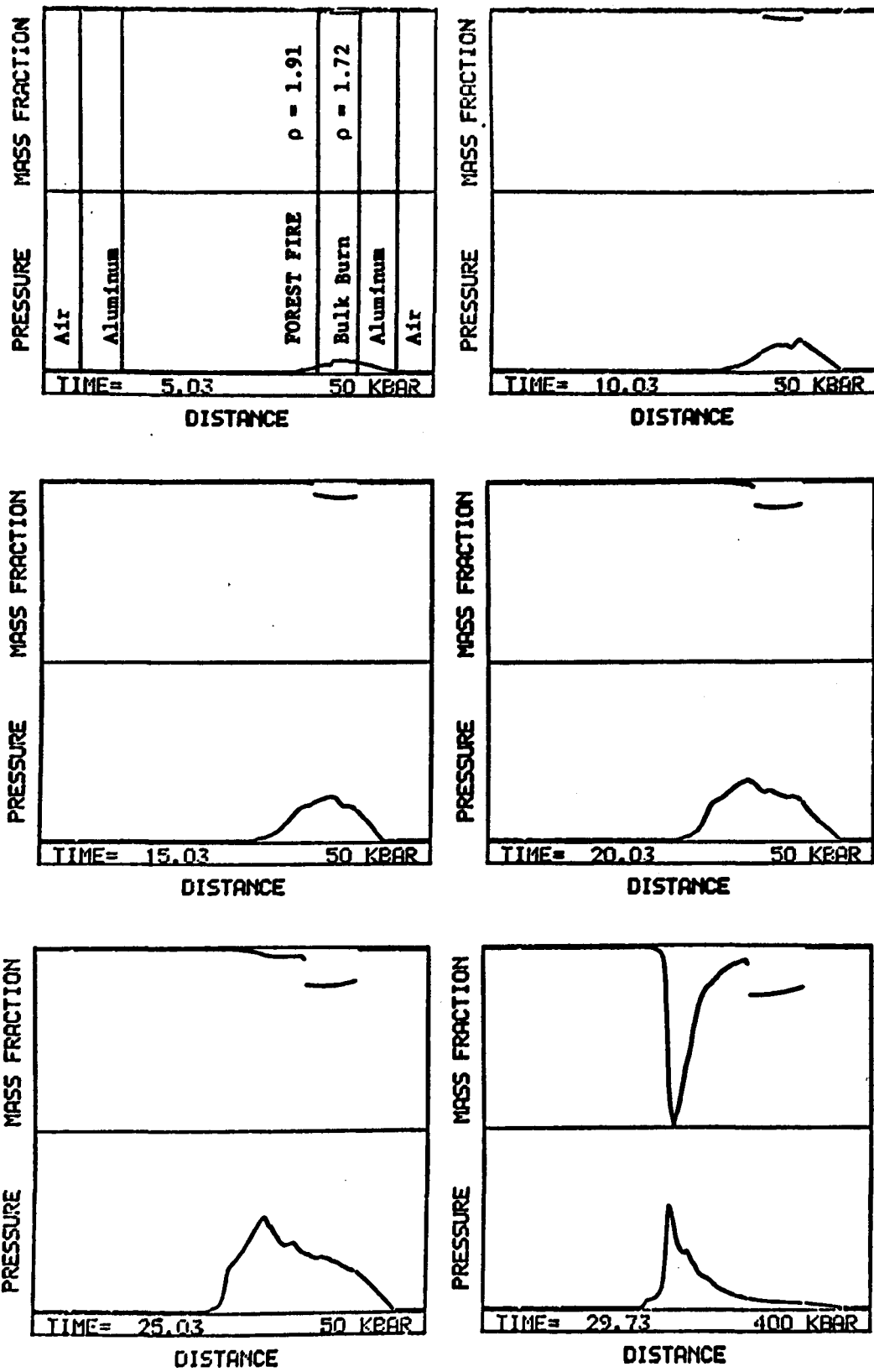


Fig. 4d.
SIN calculation for a 1-D plane in problem geometry II with $(S/V)_0 = 100/\text{cm.}$

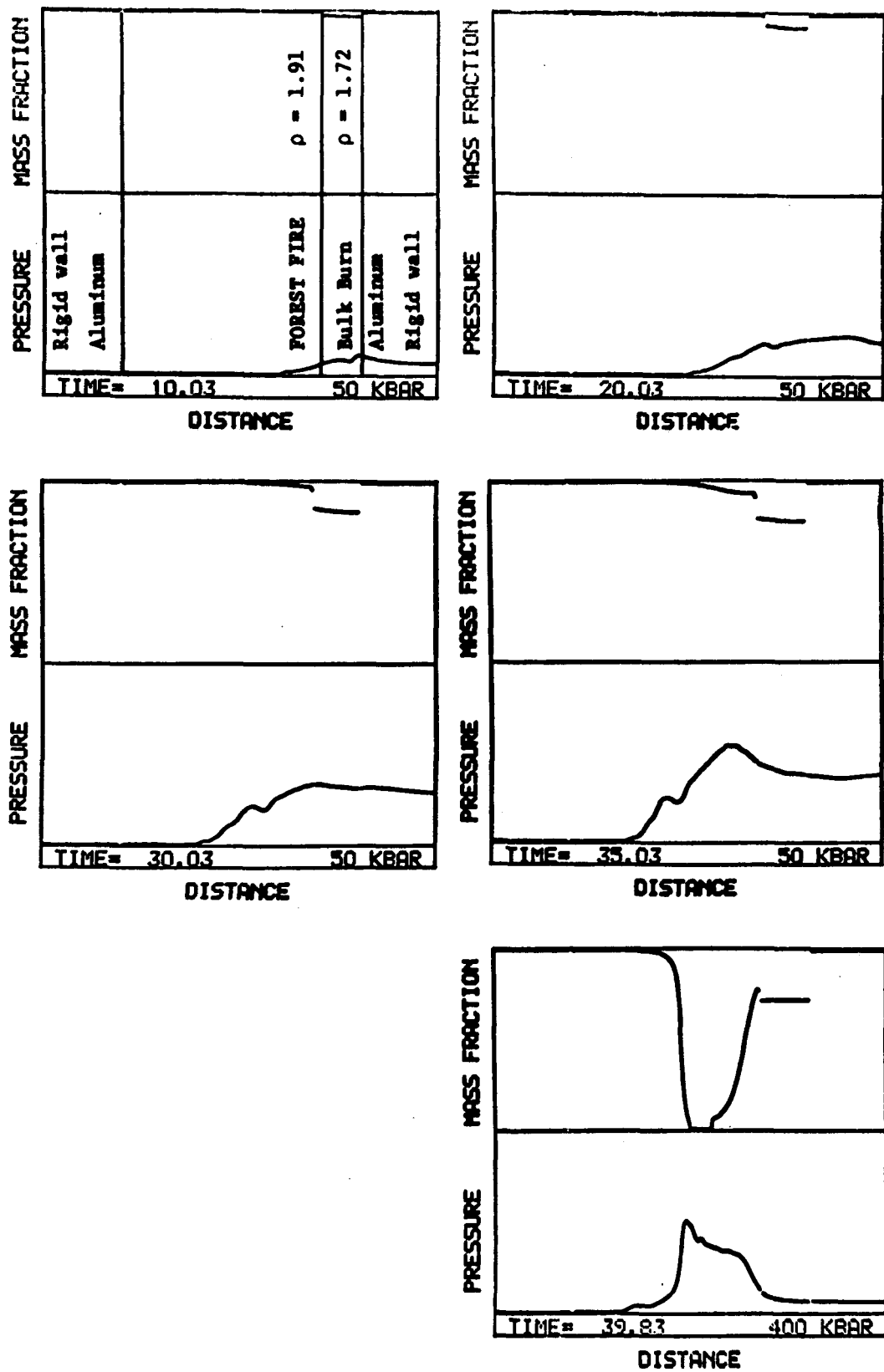


Fig. 4e.
SIN calculation for a 1-D plane in problem geometry I with $(S/V)_0 = 75/\text{cm}.$

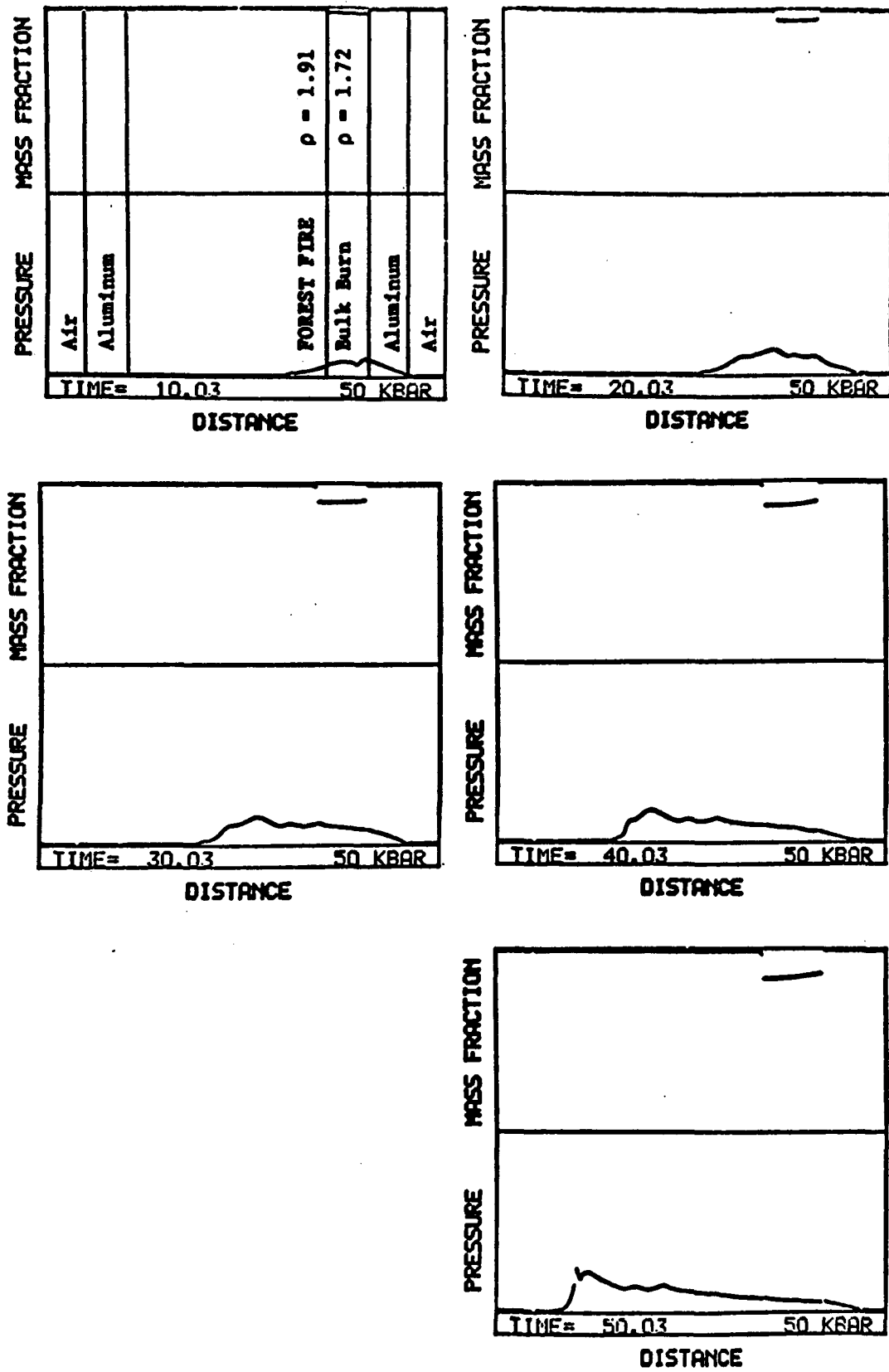


Fig. 4f.
SIN calculation for a 1-D plane in problem geometry II with $(S/V)_0 = 75/\text{cm}.$

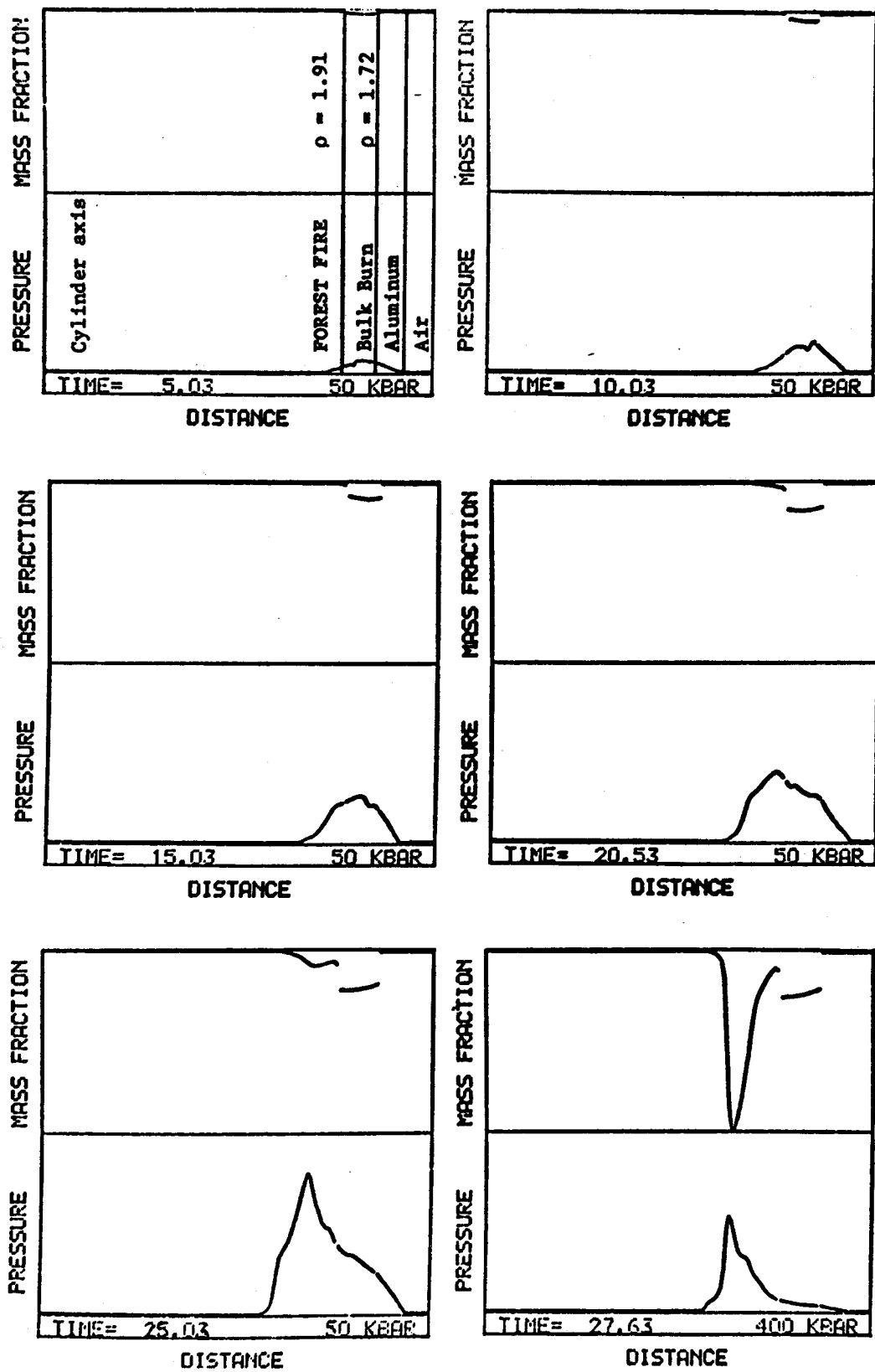


Fig. 4g.

SIN calculation for a 1-D cylinder in problem geometry III with $(S/V)_0 = 100/\text{cm}^3$.

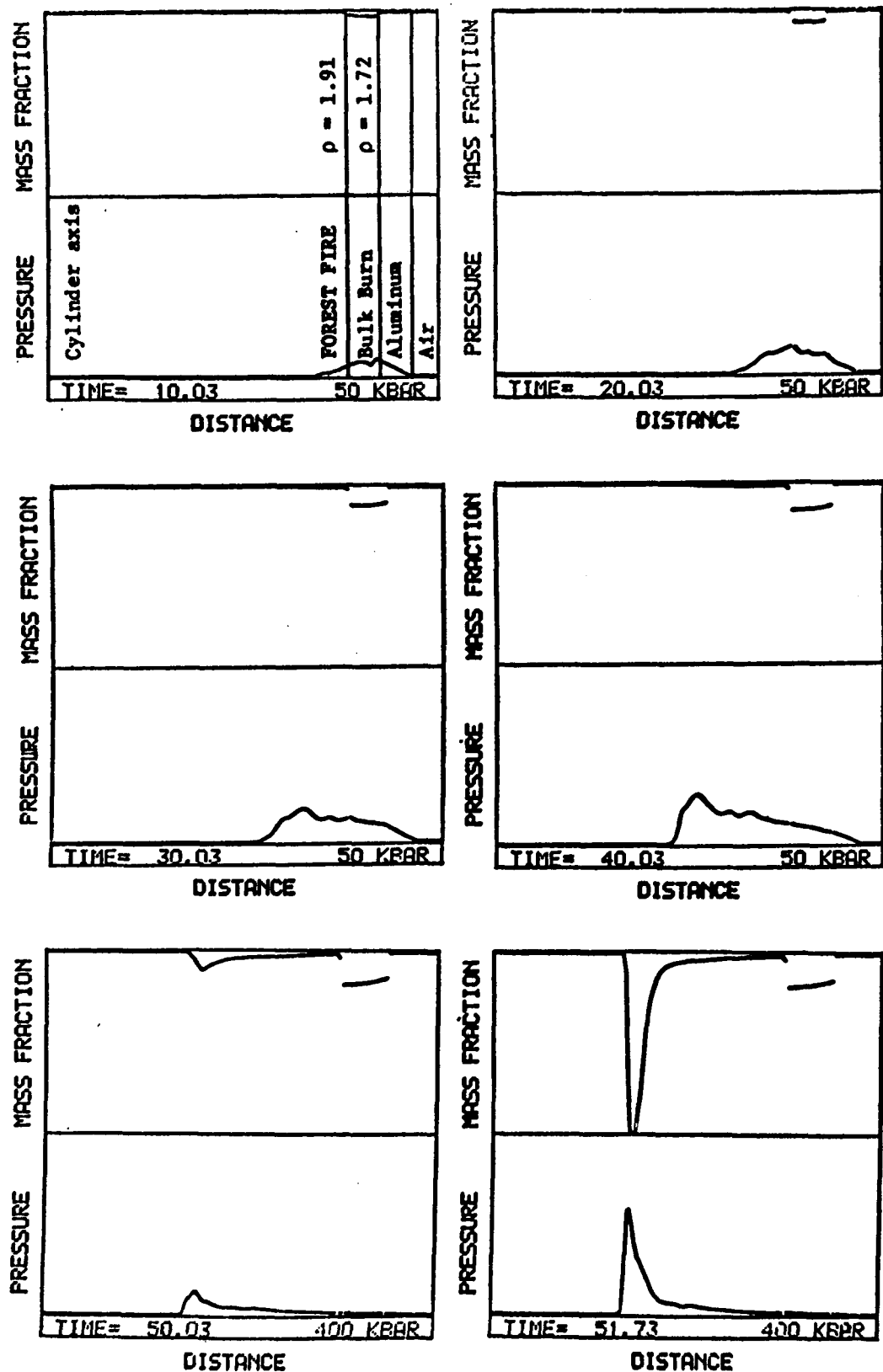


Fig. 4h.
SIN calculation for a 1-D cylinder in problem geometry III with $(S/V)_0 = 75/\text{cm}^3$.

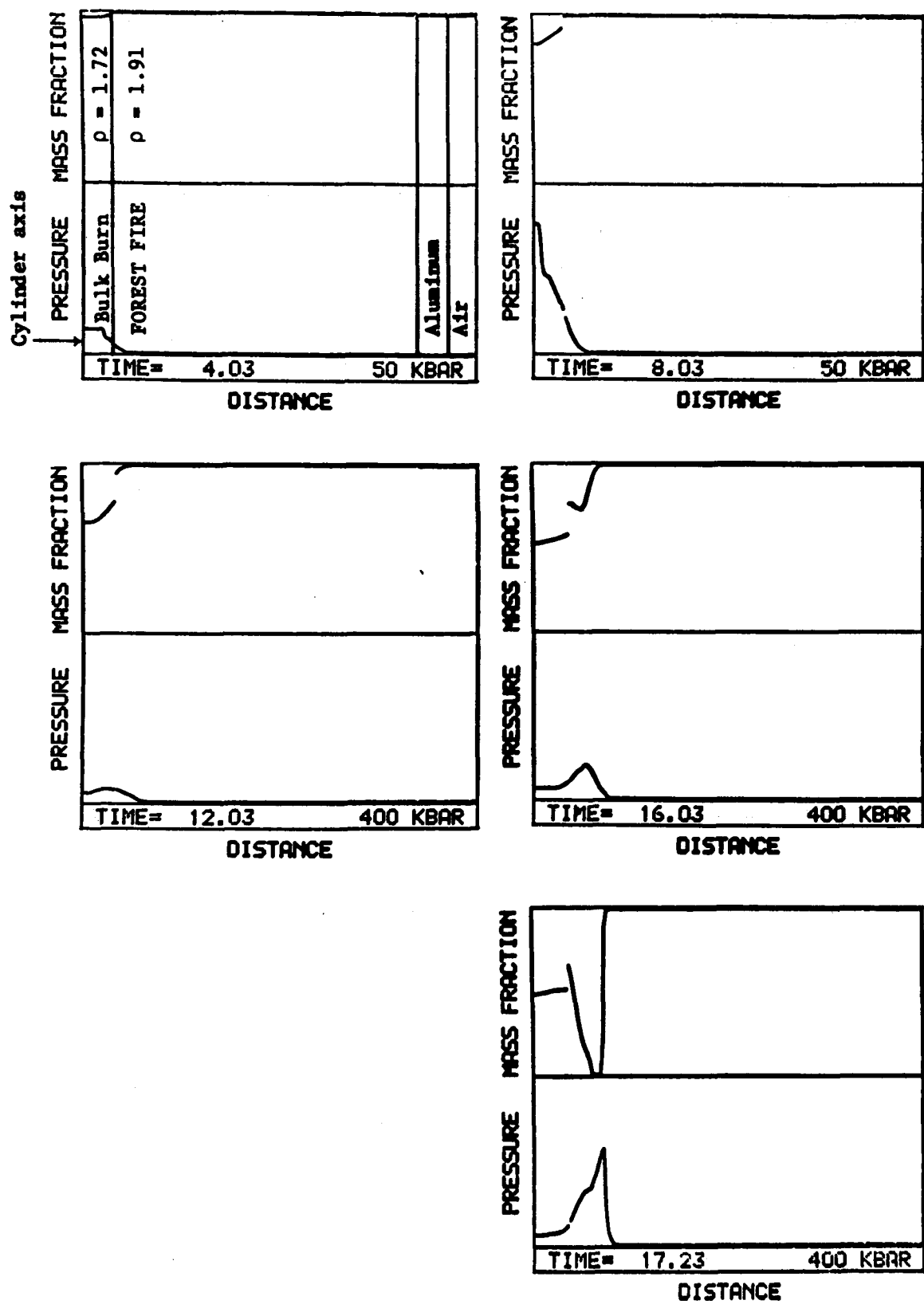


Fig. 4i.
SIN calculation for a 1-D cylinder in problem geometry IV with $(S/V)_0 = 200/\text{cm}^3$.

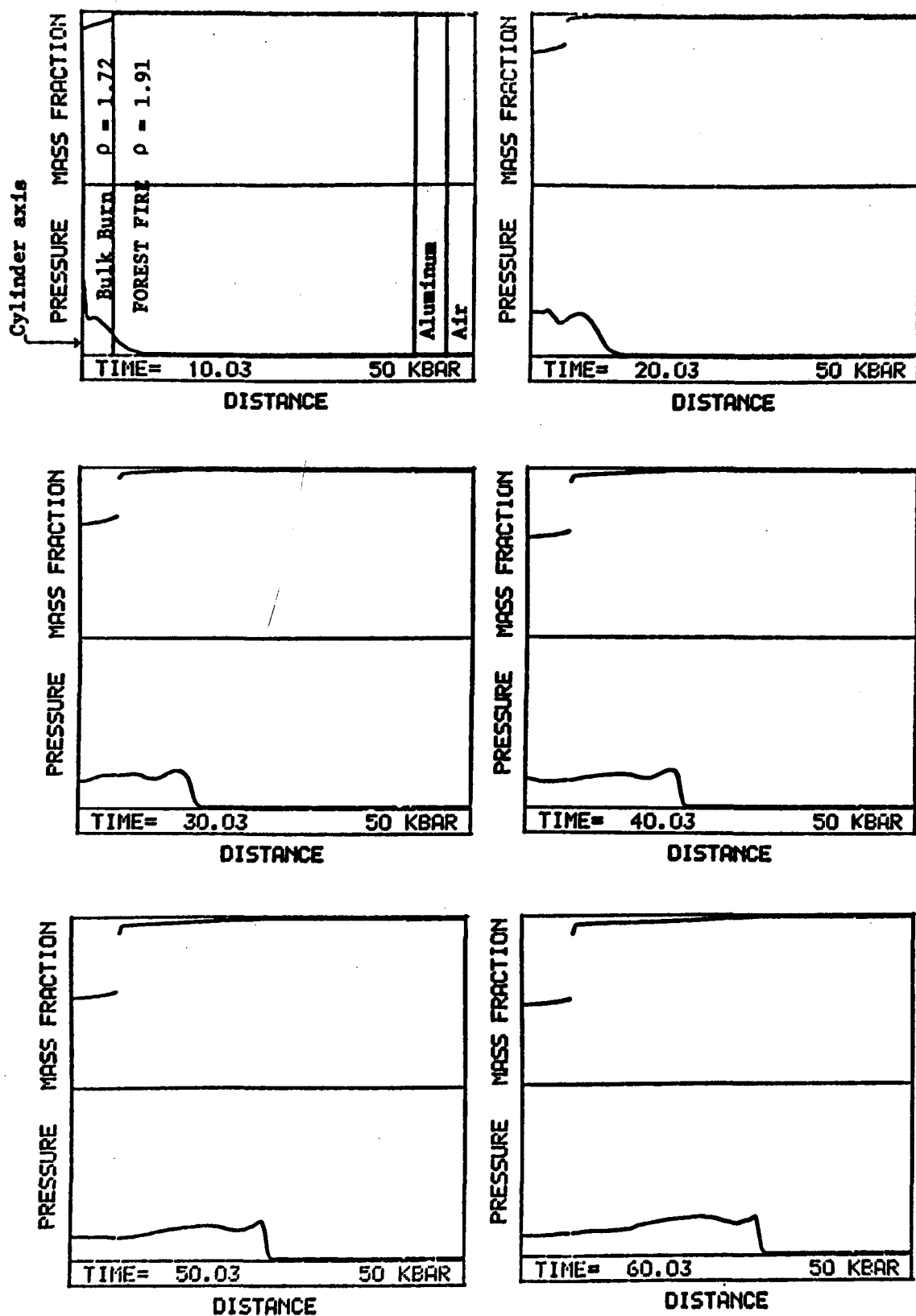


Fig. 4j.
SIN calculation for a 1-D cylinder in problem geometry IV with $(S/V)_0 = 130 \text{ cm.}$

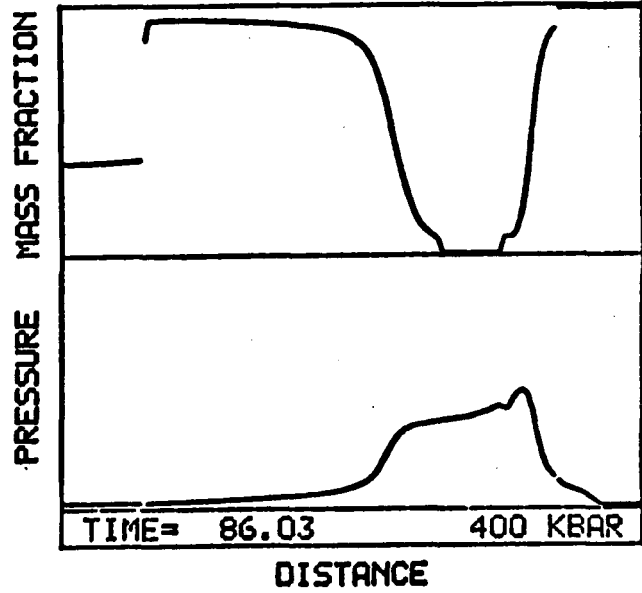
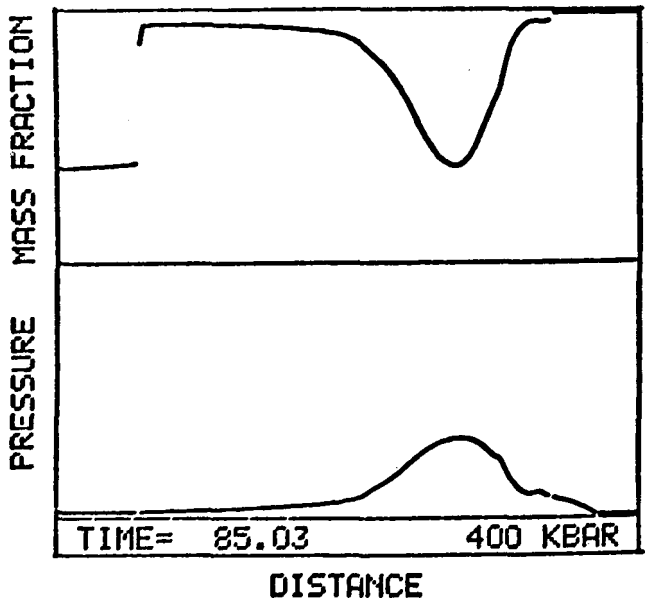
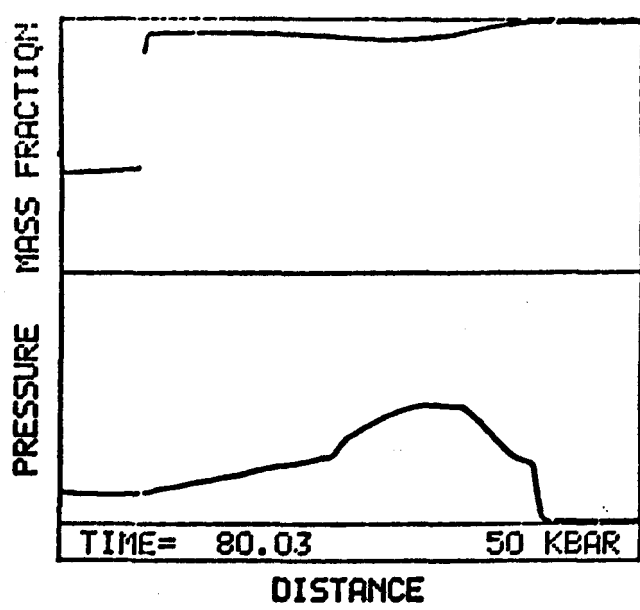
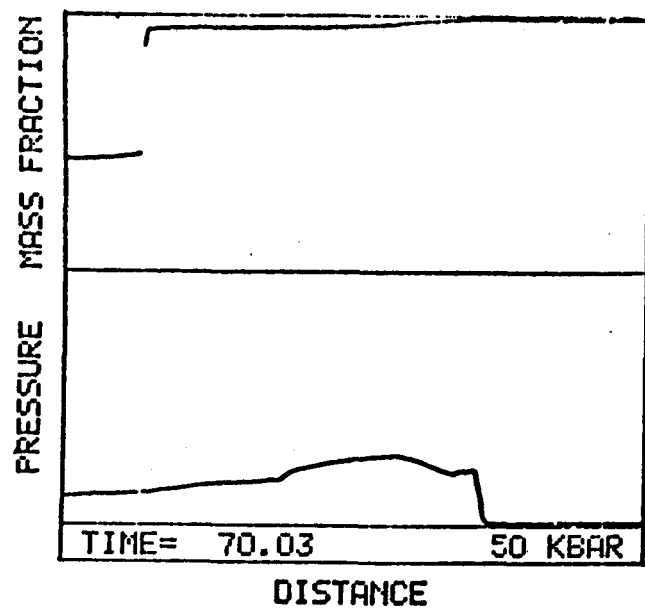


Fig. 4j. (cont)

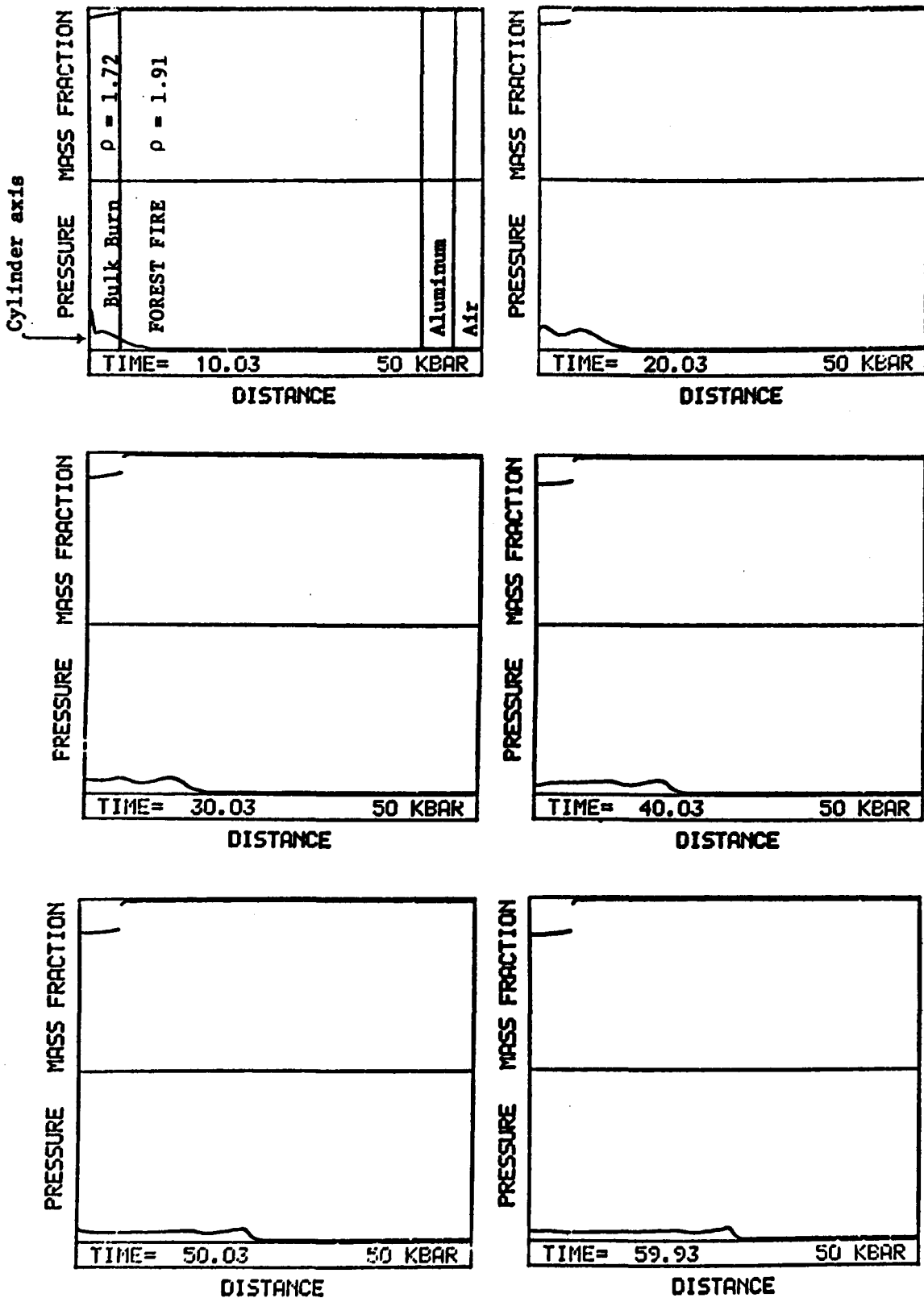


Fig. 4k.
 SIN calculation for a 1-D cylinder in problem geometry IV with $(S/V)_0 = 100/\text{cm}^3$.

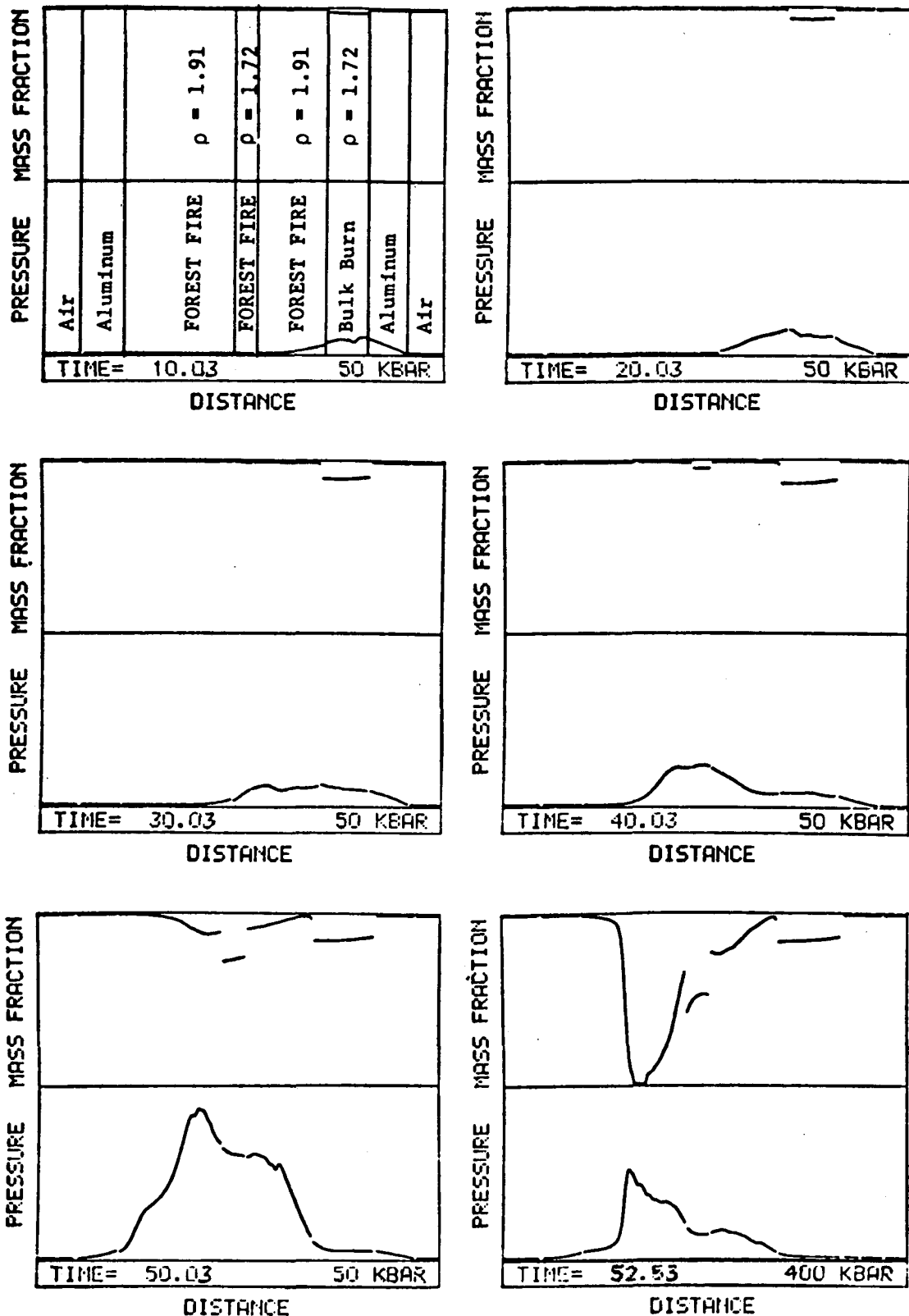


Fig. 4 ℓ .
 SIN calculation for a 1-D plane in problem geometry V with $(S/V)_0 = 75/\text{cm.}$

IV. CONCLUSIONS

This study has examined some of the conditions leading to detonation in a solid explosive bounded by a confined porous burning region. Items important to occurrence of detonation are (1) the surface area burning, (2) the confinement of the burning region, (3) the geometry of the system, and (4) the shock sensitivity of the adjacent solid material. Items (1)-(3) work together to produce the pressure waves that generate shocks in the solid. Geometry is especially critical here; a system which may not produce detonation in planar geometry may well induce detonation in converging geometry. Finally, the solid material shock sensitivity determines the response to the shocks generated. Indeed, the planar geometries (II) and (V) with $(S/V)_0 = 75/\text{cm}$ illustrate this effect well. Note that only a portion of the solid explosive adjacent to the burning region need be more sensitive to go from a nondetonating condition to a detonating one.

ACKNOWLEDGMENTS

I gratefully acknowledge the contributions of Charles L. Mader, Bobby G. Craig, Jerry D. Wackerle, and Louis C. Smith, all at the Los Alamos Scientific Laboratory.

APPENDIX A

BULK BURN

The bulk burn model is used to simulate the burning of a porous bed of explosive that is assumed to be ignited over all burning surfaces simultaneously. The explosive is assumed to be divided into uniform pieces of similar geometry that burn at the linear burn rate perpendicular to the surface of each particle. The change in burning surface area as the particles are consumed is included. The model for surface area change is motivated by three special geometric situations: (1) sphere-like particles, volumes that contain an inscribed sphere; (2) cylinder-like particles, volumes that contain an inscribed cylinder; and (3) sheet-like particles, volumes that have constant surface area. In the first two cases the surface area and volume of the particles are functions of the radius of the inscribed sphere or cylinder only. In all three cases there exists a q so that $(\text{surface area}/\text{initial surface area}) = (\text{volume}/\text{initial volume})^q$ with $q = 2/3$ for sphere-like, $q = 1/2$ for cylinder-like, and $q = 0$ for sheet-like particles. However, q may assume any value to simulate mixtures of particle types.

Bulk burn is a simplified treatment of the process known as convective combustion, in which hot gases from the burn flow into the porous bed ahead of the burning region. The flowing hot gases heat the cold particles until ignition and enter into the fluid dynamics (two-phase flow). In spite of the simplifications, bulk burn is appropriate for small confined regions where gas motion during ignition and burning is small.

BULK BURN MODEL

Notation:

Vol = volume of particle

V = volume of solid

M = mass of the solid

W = (M/M_0) = mass fraction of solid

ρ = density of solid

S = surface area burning

\dot{X} = linear burn rate = cP^n

q = "geometric" constant

The subscript zero (for example, V_0) denotes initial values.

Model Relations and Assumptions:

Each particle is assumed to burn at a linear rate $\dot{X} = dx/dt$ perpendicular to its surface. Thus the time derivative of mass burning is

$$\frac{dM}{dt} = -S\rho\dot{X} .$$

Model Development:

To isolate (S_0/V_0) in the model, expand dM/dt as follows:

$$\frac{dM}{dt} = S\rho\dot{X} ,$$

$$\frac{dM}{dt} = -(S_0/V_0)(S/S_0)(\rho_0 V_0)(\rho/\rho_0)\dot{X} .$$

The term (S/S_0) above is a function of time and needs to be related to the mass. For this purpose let

$$(S/S_0) = (\rho V/\rho_0 V_0)^q (\rho/\rho_0)^{-q} = W^q (\rho/\rho_0)^{-q} .$$

(The motivation for this will be discussed on p. 21.)

Substitution of this expression into the equation above gives

$$\frac{dW}{dt} = -(S_0/V_0)(\rho/\rho_0)^{1-q} W_X^{q_0} .$$

The constant q has value

- $q = 0$ for sheet-like particles,
- $q = 1/2$ for cylinder-like particles,
- $q = 2/3$ for sphere-like particles.

Motivation for $(S/S_0) = (M/M_0)^q (\rho/\rho_0)^{-q}$

An assumption of bulk burn is that each particle burns perpendicular to its surface. For certain polyhedral particles this assumption implies that the "shape" of the particle is fixed as the particle burns. Consider now the following three cases of special polyhedral particle shapes.

For sphere-like polyhedra (containing an inscribed sphere of radius r), the surface and volume relations are

$$S = Ar^2 , \quad Vol = Ar^3/3 , \quad \text{and}$$

$$(S/S_0) = (r/r_0)^2 = (Vol/Vol_0)^{2/3} ,$$

where A is a constant. (For example, for a cube $A = 24$.)

For cylinder-like polyhedra (containing an inscribed cylinder of radius r and ignoring the surface area of the ends), the relations are

$$S = Ar\ell , \quad Vol = Ar^2\ell/2 , \quad \text{and}$$

$$(S/S_0) = (r/r_0) = (Vol/Vol_0)^{1/2} ,$$

where ℓ is the length of the particle and A is a constant. (For example, for a square tube, $A = 8$.)

For plane-like volumes with constant surface area, the relations are

$$S = S_0 \quad \text{and}$$

$$(S/S_0) = 1 = (Vol/Vol_0)^0 .$$

In each of the above cases

$$(S/S_0) = (Vol/Vol_0)^q , \quad \text{for some } q .$$

Thus

$$(S/S_0) = (\rho V_{01}/\rho_0 V_{01})^q (\rho/\rho_0)^{-q}$$

and finally

$$(S/S_0) = (M/M_0)^q (\rho/\rho_0)^{-q} .$$

APPENDIX B

SHOCK INITIATION AND THE POP-PLOT

I. INTRODUCTION

The phrase "shock initiation of high explosive" refers to the process in which a shock wave passing through a piece of explosive material grows into a detonation wave. This process has been studied extensively in "sensitivity tests." One such test which has been a favorite for years and which, because of its one-dimensionality, is of special interest is the "wedge test." In this test, a wedge of high explosive is placed on a large planar shock-wave generator and the distance that the shock runs through the wedge before detonation occurs is observed with a streak camera. The change to detonation is marked by a rapid change in the shock velocity. A sequence of such shots with varying initial shock pressure in the explosive defines a graph of distance to detonation versus initial shock pressure. This graph is often a straight line in $(\log P, \log \text{run})$ coordinates and is known as the POP-PLOT (after Alphonse Popolato). The wedge test also furnishes the time to detonation, initial particle velocity (U_p), and initial shock velocity (U_s). The (U_p, U_s) line is known as the Hugoniot for the material.

The POP-PLOT and Hugoniot data have been used to describe and compare shock sensitivity of heterogeneous explosives. Also the data have been incorporated into a model of shock-induced decomposition rate in heterogeneous explosive called FOREST FIRE.¹ The model uses an assumption known as "single curve build-up," which asserts that during shock initiation the pressure wave grows along a unique line in (time, distance, state) space. The POP-PLOT is interpreted in the FOREST FIRE model to be that unique shock growth line, even though it is not what the wedge test actually measures.

The FOREST FIRE model addresses the question: What decomposition rate in the flow behind the shock is consistent with shock growth along the POP-PLOT line? The shock is assumed to have a square wave front ($\partial P/\partial X \equiv 0$) to complete the data necessary for solution (note that if the pressure is known throughout the material, the entire flow may be analyzed to give decomposition rates). The HOM equation of state is used for the mixture of solid and decomposition products. As a setting for the later discussion of POP-PLOT calculation, a brief outline of the analysis as restricted to the shock front only is given. A more detailed and more general account is found in Ref. 1.

Note now that in this model the decomposition rate is calculated along one curve in state space, namely a single shock Hugoniot. At each point of this line are calculated the state variables P , V , I , T , W , U_p , and rate, $-(dW/dt)/W$. The representation of the rate as a function of these state variables is not uniquely determined. It may be a function of several of the variables or their derivatives. However, after some experimentation with various forms, representation of rate as a function of pressure only was found to be convenient and fairly successful. No claim is made that the rates are necessarily pressure dependent nor that FOREST FIRE is a pressure-dependent rate-law model. When information becomes available about the rate process off the single shock Hugoniot or as cases arise for which the pressure-dependent rate is not applicable, the matter will need to be considered again.

In the model description, "Model Relations" are the equations that express the various assumptions used in constructing the model. They are stated separately before being incorporated into the "Solution Method" that follows. This notation is used throughout the development.

P = pressure (Mbar)

U_p = particle velocity (cm/ μ s)

Also, $U = U_p$ (written without the subscript p)

V = specific volume (cm 3 /g)

I = specific internal energy (Mbar cm 3 /g)

W = mass fraction of undecomposed explosive

$W = 1$, all undecomposed explosive

$W = 0$, all decomposition products

r_{run} = distance to detonation (cm)

t_{det} = time to detonation (μ s)

For any function $f = f(m, \tau)$,

$$f_m = \frac{\partial f}{\partial m} \quad \text{and} \quad f_\tau = \frac{\partial f}{\partial \tau} .$$

Similarly, for $H = H(V, I, W)$

$$H_V = \frac{\partial H}{\partial V} , \quad H_I = \frac{\partial H}{\partial I} , \quad \text{and} \quad H_W = \frac{\partial H}{\partial W} .$$

II. FOREST FIRE RATE CALCULATION

The shock is assumed to grow in pressure as it moves through distance according to POP-PLOT, relations (1) and (2). The shock is taken to be a sharp shock on the $U_s = C + S U_p$ line, relation (3). This Hugoniot line may be the inert Hugoniot or a reactive Hugoniot. (In Fig. A-1 are illustrated an inert and a reactive Hugoniot³ for PBX 9404.) Relation (4) expresses that, in the region behind the shock, an equation of state (for example, HOM) describes the mixture of unreacted explosive and reaction products.

MODEL RELATIONS

FOREST FIRE RATE CALCULATION

- (1) POP-PLOT: $\ln(\text{run}) = a_1 + a_2 \ln(P - a_3)$
- (2) Interpret POP-PLOT using
SINGLE CURVE BUILD-UP HYPOTHESIS.

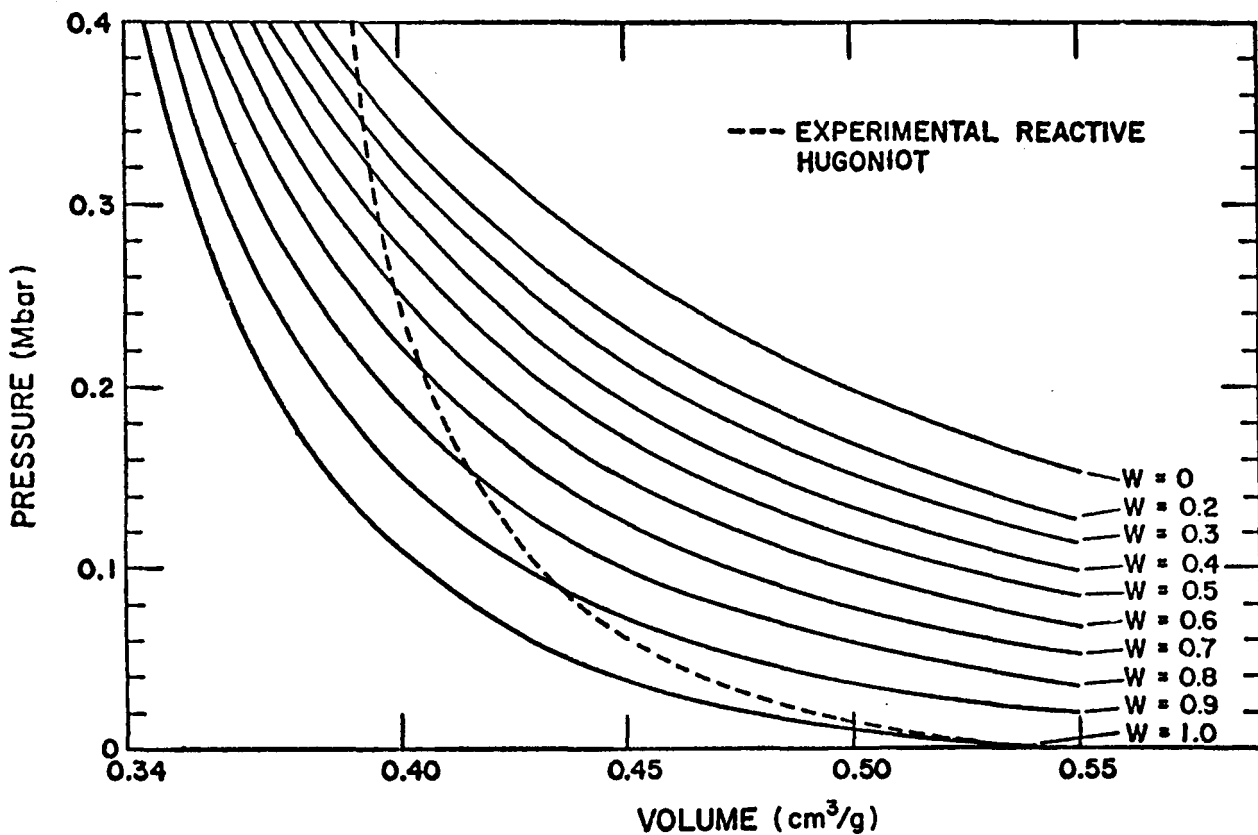


Fig. A-1.
HOM equation-of-state partial reaction Hugoniots at various mass fraction of solid (W) for PBX 9404. The dashed line is the experimental "reactive" Hugoniot of Ramsay and Popolato (Ref. 3). The W = 1.0 line is the solid "inert" Hugoniot.

$$(3) \text{ Hugoniot: } U_s = C + S U_p$$

$$P = \rho_0 U_s U_p$$

$$V = V_0 (U_s - U_p) / U_s$$

$$I = U_p^2 / 2$$

$$(4) \text{ Equation of State: } P = H(V, I, W) \quad (\text{HOM equation of state})$$

Briefly, the HOM equation of state² gives pressure as a function of the specific volume and specific internal energy of the mixture of solid and gaseous products and of the mass fraction of solid. The solid equation of state is expanded off the Hugoniot with the Grüneisen construction that has a constant gamma (Γ). The gas is expanded off the detonation product isentrope. The mix rule assumes ideal mixing of specific volumes of solid and gas and energy partitioning according to mass fraction. Pressure and temperature equilibrium are required, and solution for V_s and V_g is obtained.

HOM EQUATION-OF-STATE RELATIONS (Ref. 2)

Equation of State:

$$P = H(V, I, W)$$

V = specific volume

I = specific internal energy

W = mass fraction of undecomposed explosive

Grüneisen solid equation of state:

$$(U_s = C + S U_p)$$

$$P_s = \Gamma (I_s - I_H) / V_s + P_H$$

$$T_s = (I_s - I_H) \cdot 23890 / C_{v,s} + T_H$$

Gas Equation of State: (BKW isentrope)

$$P_g = (I_g - I_i) / (\beta V_g) + P_i$$

$$T_g = (I_g - I_i) 23890 / C_{v,g} + T_i$$

Mix Rule: Pressure and temperature equilibrium

$$P_s(V_s) = P_g(V_g) \text{ and } T_s(V_s) = T_g(V_g)$$

with

$$V = WV_s + (1 - W)V_g$$

$$I = WI_s + (1 - W)I_g$$

Regular one-dimensional planar fluid flow is assumed behind the shock, relation (5). The shock is accelerating and is differentiated in time, relation (6). At each mass point the equation of state applies and is differentiable with respect to time, relation (7). With the additional information about the pressure gradient behind the shock, the solution for W_τ is possible.

MODEL RELATIONS

FOREST FIRE RATE CALCULATION (cont)

(5) Fluid Flow: Lagrange mass coordinates (m, τ)

$$\frac{\partial}{\partial m} = \frac{1}{\rho} \frac{\partial}{\partial x} \text{ and } \frac{\partial}{\partial \tau} = \frac{\partial}{\partial t} + U \frac{\partial}{\partial x}$$

$$U_\tau = -P_m$$

$$V_\tau = U_m$$

$$I_\tau = -PV_\tau$$

(6) Shock Front Derivatives:

$$\frac{\circ}{P} = \frac{dP[X_s(t), t]}{dt}$$

X_s = shock position

$$\frac{\circ}{P} = \rho_0 U_s P_m + P_\tau$$

$$\frac{\circ}{U} = \rho_0 U_s U_m + U_\tau$$

$$\frac{\circ}{P} = (dP/d \text{ run}) U_s$$

$$\frac{\circ}{U} = \frac{\circ}{P} V_0 / (C + 2SU)$$

(7) Total Derivative of Equation of State:

$$P_{\tau} = H_V \cdot V_{\tau} + H_I \cdot I_{\tau} + H_W \cdot W_{\tau}$$

The solution method consists of solving for the time derivatives P_{τ} , V_{τ} , and I_{τ} behind the shock from the time derivatives of the shock front. The pressure gradient at the shock front is taken to be zero if this information is not known explicitly. (Under such circumstances the solution method solves a shock with a "square" leading edge.) The state of the front is determined by the POP-PLOT and shock jump relations. The total derivative of the equation of state allows for solution of W_{τ} if $\partial H / \partial W \neq 0$. The solution thus is outlined in (A), (B), and (C).

SOLUTION METHOD

FOREST FIRE RATE CALCULATION

Let P be the independent variable.

(A) Solve the shock front state.

$$\text{Calculate run, } \text{run} = \exp [a_1 + a_2 \ln(P - a_3)] .$$

$$\text{Solve for } U_p, \quad P = \rho_0 (C + S U_p) U_p .$$

$$\text{Calculate } U_s = C + S U_p$$

$$V = V_0 (U_s - U_p) / U_s$$

$$I = U_p^2 / 2 .$$

$$\text{Solve for } W, \quad P = H(V, I, W) .$$

(B) Solve for Lagrangian time derivatives P_{τ} , V_{τ} , and I_{τ} behind the shock.

$$\text{Calculate } \overset{\circ}{P} = (dP/d \text{run}) U_s$$

$$\overset{\circ}{U} = \overset{\circ}{P} V_0 / (C + 2 S U) .$$

Assume $P_m \equiv 0$, if pressure gradient information is not available.

$$\text{Calculate } P_{\tau} = \overset{\circ}{P} - \rho_0 U_s P_m$$

$$V_{\tau} = (\overset{\circ}{U} + P_m) / (\rho_0 U_s)$$

$$I_{\tau} = -P V_{\tau} .$$

(C) Solve for W_T ,

$$P_T = H_V V_T + H_I I_T + H_W W_T .$$

III. POP-PLOT CALCULATION

The shock sensitivity of an explosive is greatly influenced by the initial density of the explosive. For example, an explosive pressed to low density is more sensitive than if it were pressed to high density. Correspondingly, the POP-PLOT reflects the change in sensitivity for different densities. A method is given here to estimate the POP-PLOT change with density given a POP-PLOT at some initial reference density.

The method of POP-PLOT calculation uses the assumption that the shock particle velocity as a function of time to detonation is independent of density. The assumption is based upon the observation that this seems to be true for PBX 9404 and PETN (see Fig. A-2). Also, the single curve build-up assumption is employed to interpret the POP-PLOT at the reference density. The shock Hugoniot at other densities is constructed using the Grüneisen form of the equation of state.⁴ The function $U_p(t_{det})$ is obtained from the wedge test data.

Note here that the assumption about $U_p(t_{det})$ may not necessarily hold for all explosives. An examination of this matter may be important in developing further theories about initiation.

Figures A-2 through A-5 show the input curves of $U_p(t_{det})$, the calculated POP-PLOTS, and calculated time-to-detonation, distance-to-detonation curves, all with the experimental points. The data for PBX 9404 are from B. G. Craig.⁵ The PETN data for $\rho = 1.75$ are from J. D. Wackerle.⁶ The PETN data for $\rho = 1.72$ and $\rho = 1.60$ are from D. Stirpe et al.,⁷ and the data for PETN $\rho = 1.0$ are from G. E. Seay and L. B. Seely.⁸ The curves are calculated from the $U_p(t_{det})$ line and the Hugoniot of the highest density for each explosive.

Model relations for POP-PLOT calculation are listed below. Relation (1) states that U_p is independent of time to detonation and that the Hugoniot for the solid at density ρ_1 is as measured. Relation (2) is the Grüneisen construction of the Hugoniot at density ρ_2 .

MODEL RELATIONS

POP-PLOT CALCULATION

$$(1) \text{ Data at } \rho_1 \quad \begin{cases} U_p(t_{det}) = F(t_{det}) \\ U_s = C + S U_p \end{cases}$$

$$(2) \text{ Grüneisen Equation-of-State Construction of Hugoniot at } \rho = \rho_2 \text{ (Ref. 4)}$$

$$P = \Gamma(I - I_H)/V + P_H$$

with

$$I = 0.5 P(V_2 - V)$$

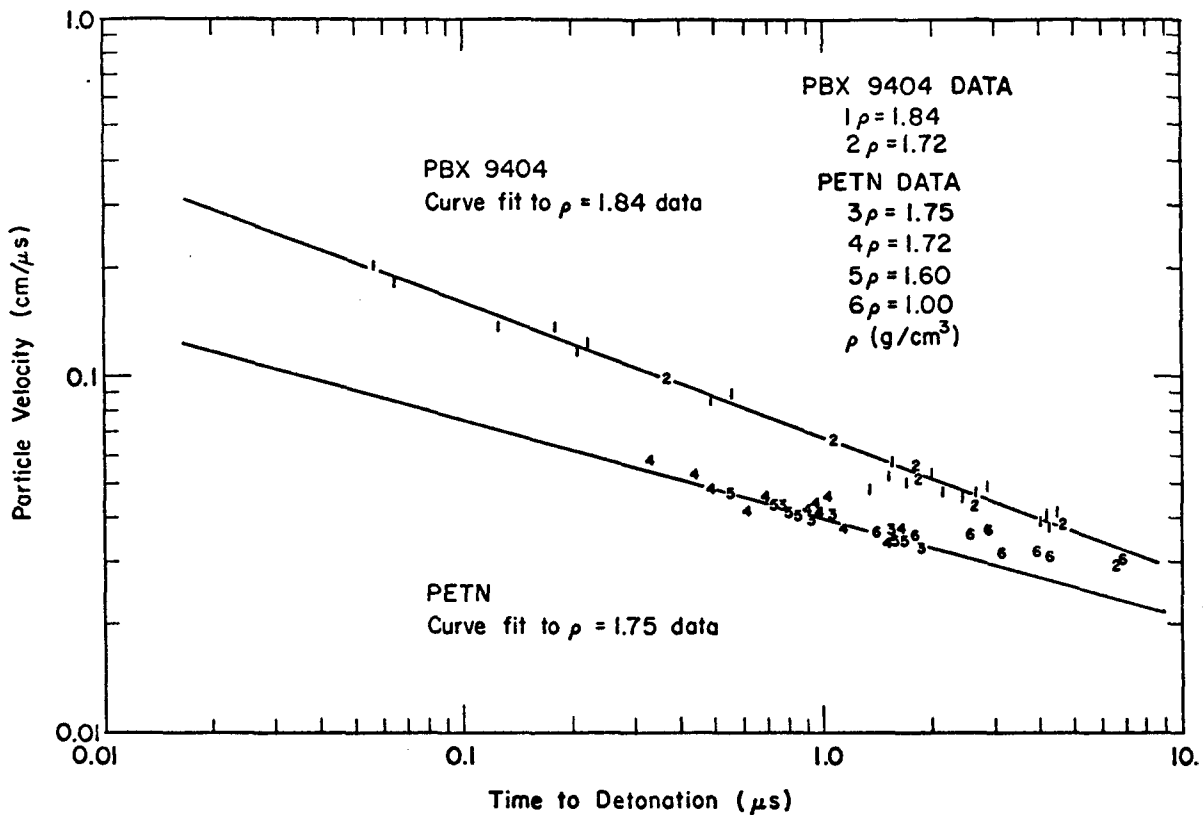


Fig. A-2.
Shock particle velocity vs time to detonation showing the invariance of the graph with different densities.

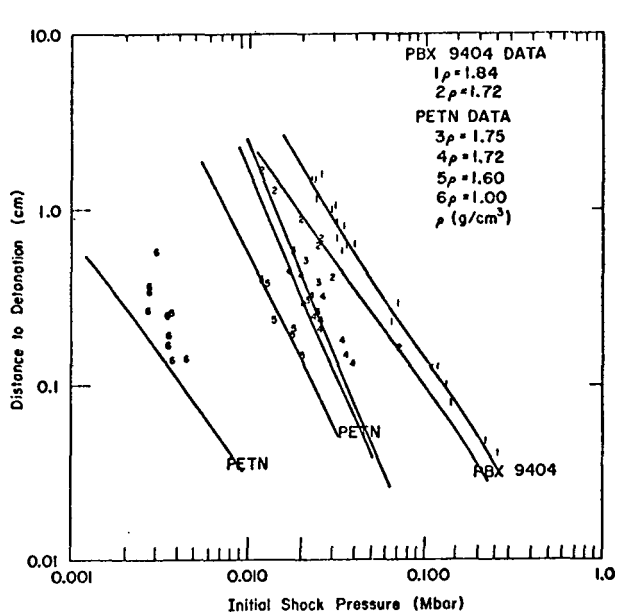


Fig. A-3.
Calculated POP-PLOTS for PBX 9404 and PETN. The lines are calculated from the data at the highest density for each explosive.

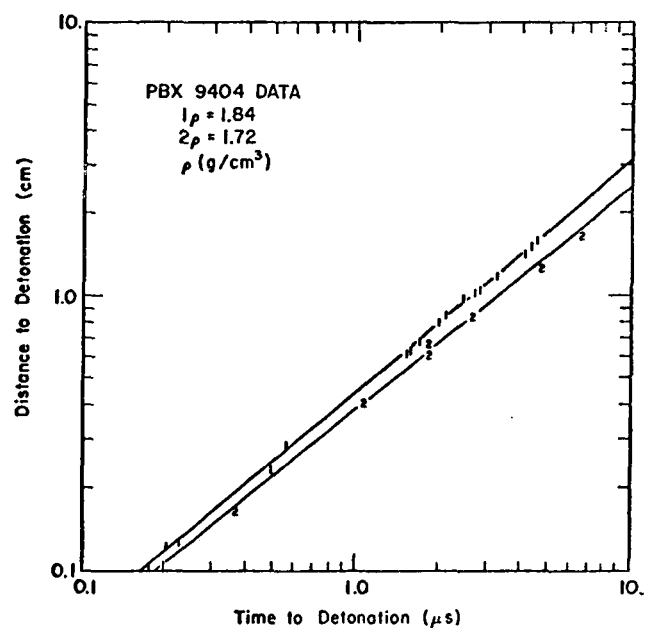


Fig. A-4.
Calculated distance to detonation vs time to detonation for PBX 9404 based on the data at $\rho = 1.84$.

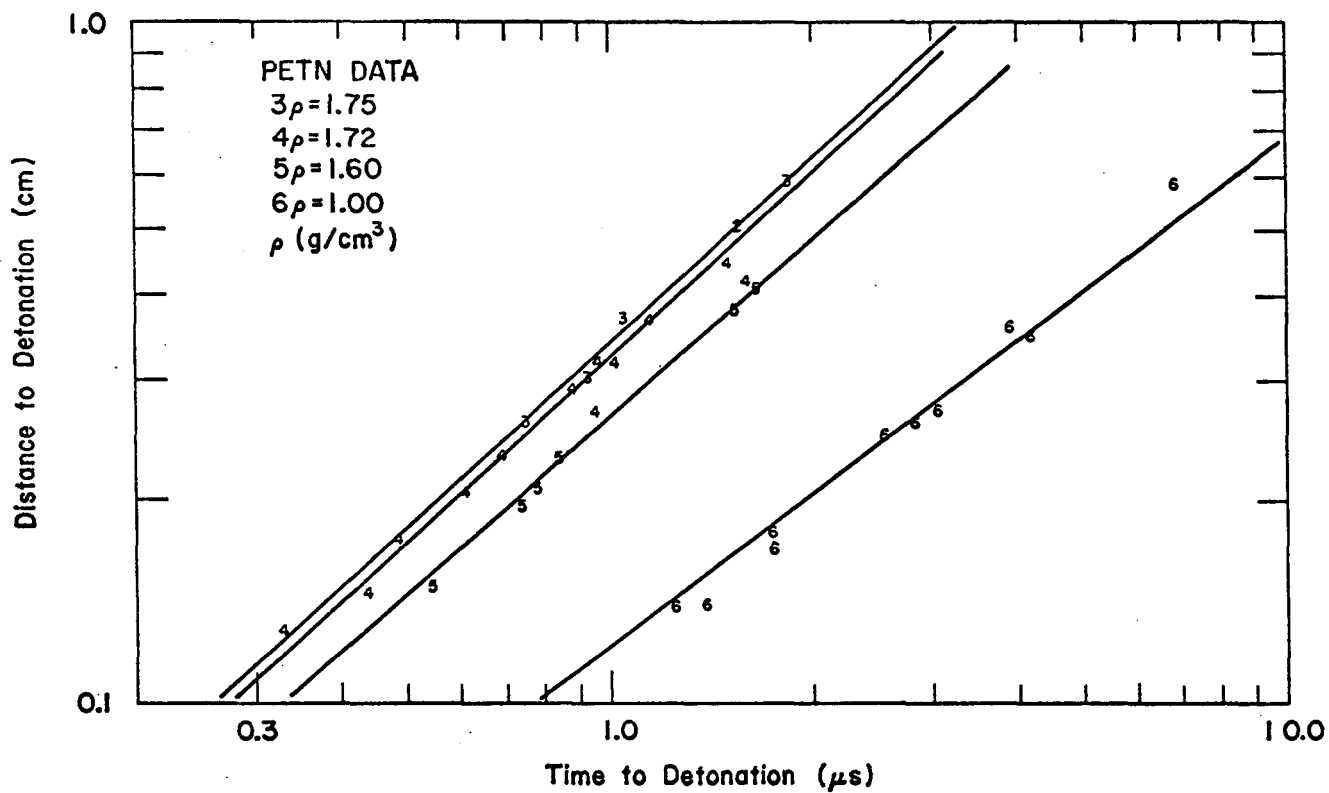


Fig. A-5.

Calculated distance to detonation vs time to detonation for PETN based on the data at $\rho = 1.75$.

$$I_H = 0.5 P_H (V_1 - V)$$

$$P_H = C^2 (V_1 - V) / [V_1 - S(V_1 - V)]^2$$

Then

$$P = P_H(V)G(V) ,$$

where

$$G(V) = [2V - \Gamma(V_1 - V)] / [2V - \Gamma(V_2 - V)] .$$

The solution method uses the shock pressure as the independent variable. From the constructed Hugoniot, solution is made for the specific volume, particle velocity, and shock velocity. Using the assumption about $U_p(t_{det})$ being independent of density, solution is made for time to detonation. Finally the shock velocity is integrated to give distance to detonation.

SOLUTION METHOD

POP-PLOT CALCULATION

Input Data: $[U_p(t), U_s = C + S U_p]$

Let P be the independent variable.

Solve for V ,

$$P = P_H(V)G(V) .$$

Then

$$U_p = [P(V_2 - V)]^{1/2}$$

$$U_s = V_2 [P/(V_2 - V)]^{1/2} .$$

Assume $U_p(t_{det}) = F(t_{det})$, independent of ρ , and calculate t_{det} .

Finally after a table of (t_{det}, U_s) is formed,

$$\text{run} = \int_0^{t_{det}} U_s dt' .$$

IV. POP-PLOT AND FOREST FIRE RATE CALCULATION

Often the particle velocity and time to detonation for wedge tests are not reported. Rather, it seems to be customary to report only the POP-PLOT line and the Hugoniot. To compute the POP-PLOT and FOREST FIRE rates for another density then requires construction of $U_p(t_{det})$ and the shock change derivatives \dot{P} and \dot{U}_p . Given here is a method that uses the invariance of $U_p(t_{det})$ with density and the single curve build-up assumption.

Model relation (1) describes the experimental data for the reference density ρ_1 . Relation (2) is again the construction of the Hugoniot at density ρ_2 . Relation (3) gives the time derivative of the shock pressure growth at density ρ_1 and is used in inverse form to calculate time to detonation.

MODEL RELATIONS

POP-PLOT AND FOREST FIRE RATE CALCULATION

$$(1) \text{ Data at } \rho_1 \left\{ \begin{array}{l} \text{POP-PLOT: } \ln(\text{run}) = \alpha_1 + \alpha_2 \ln(P - \alpha_3) \\ \text{Hugoniot: } U_s = C + S U_p \end{array} \right.$$

(2) Grüneisen Equation-of-State Construction of Hugoniot at $\rho = \rho_2$ (Ref. 4)

$$P = \Gamma(I - I_H)/V + P_H ,$$

with

$$I = 0.5 P(V_2 - V)$$

$$I_H = 0.5 P_H(V_1 - V)$$

$$P_H = C^2(V_1 - V)/[V_1 - s(V_1 - V)]^2 .$$

Then

$$P = P_H(V)G(V) ,$$

where

$$G(V) = [2V - \Gamma(V_1 - V)]/[2V - \Gamma(V_2 - V)] .$$

(3) Time Derivative of Shock Pressure on POP-PLOT Line at $\rho = \rho_1$

$$\frac{dP}{dt} = \frac{dP}{d \text{ run}} \frac{d \text{ run}}{dt} = \frac{dP}{d \text{ run}} U_s ,$$

where

$$\frac{dP}{d \text{ run}} = (P - \alpha_3)/[\alpha_2 \text{ run}(P)]$$

and

$$U_s = 0.5[C + (C^2 + 4SV_1 P)^{1/2}] .$$

The solution method uses pressure as the independent variable. From the constructed Hugoniot, solution is for specific volume, and then particle velocity and shock velocity are calculated. Assuming $U_p(t_{det})$ is independent of density, time to detonation is determined from the data at density ρ_1 by calculating the pressure corresponding to particle velocity U_p and then integrating the inverse of the derivative relation (3). The distance to detonation is then found by integrating the constructed $U_s(t_{det})$ function.

To calculate the decomposition rates for the constructed POP-PLOT at density ρ_2 , the time derivatives for the shock are needed (see the solution method for the FOREST FIRE rate calculation given on p. 27). Here again the assumption that $U_p(t_{det})$ is independent of density is applied. From the data at ρ_1 , \dot{U}_p is calculated corresponding to the particle velocity U_p already determined. Then by differentiating the shock jump relations and the constructed Hugoniot at density ρ_2 , \dot{V} and \dot{P} are solved. Thereafter the solution method is identical to that on p. 27.

SOLUTION METHOD

POP-PLOT AND FOREST FIRE RATE CALCULATION

Let P be the independent variable.

Solve for V ,

$$P = P_H(V)G(V) .$$

Then

$$U_p = [P(V_2 - V)]^{1/2}$$

$$U_s = V_2 [P/(V_2 - V)]^{1/2}$$

$$I = 0.5 U_p^2 .$$

Assuming $U_p(t_{det})$ is independent of ρ , calculate t_{det} from the data at ρ_1 ,

$$P_1 = \rho_1(C + S U_p) U_p$$

$$t_{det} = \int_{P_1}^{P_\infty} \frac{-\alpha_2 \text{ run}(P) dP}{(P - \alpha_3) 0.5 [C + (C^2 + 4S V_1 P)^{1/2}]} ,$$

where P_∞ is the pressure so that the POP-PLOT distance to detonation is 0.0001 cm. A finite upper integration limit is used to permit numerical integration. Finally, after a table of (t_{det}, U_s) is formed,

$$\text{run} = \int_{t_{det \text{ min}}}^{t_{det}} U_s dt' .$$

Calculate the shock-induced decomposition rate for the constructed POP-PLOT.

Notation:

Let \dot{P} , \dot{U}_p , and \dot{V} be shock front derivatives with respect to time, for example

$$\dot{P} = \frac{dP[X_s(t), t]}{dt} ,$$

where X_s is the shock position.

To solve the shock change, \dot{P} and \dot{U}_p are needed.

Calculate \dot{U}_p from data at $\rho = \rho_1$, assuming

$U_p(t_{det})$ is independent of ρ

$$U_{s1} = C + S U_p$$

$$\rho_1 = \rho_1 U_p U_{s1}$$

$$\text{run1} = \exp [\alpha_1 + \alpha_2 \ln (P_1 - \alpha_3)]$$

$$\dot{P}_1 = -(P_1 - \alpha_3) U_{s1} / (\alpha_2 \text{run1})$$

$$\dot{U}_p = V_1 \dot{P}_1 / (U_{s1} + S U_p) .$$

Shock Jump Equations for $\rho = \rho_2$

$$V = V_2 (U_s - U_p) / U_s$$

$$P(V) = \rho_2 U_p U_s .$$

Differentiating with respect to time,

$$U_s \dot{U}_p = -U_s^2 \rho_2 \dot{V} + U_p \dot{U}_s$$

and

$$U_s \dot{U}_p = V_2 \frac{dP}{dV} \dot{V} - U_p \dot{U}_s ,$$

where

$$\frac{dP}{dV} = \frac{d[P_H(V)G(V)]}{dV} = \frac{dP_H}{dV} G(V) + P_H(V) \frac{dG}{dV} ,$$

$$\frac{dP_H}{dV} = \frac{-C^2 [V_1 + S(V_1 - V)]}{[V_1 - S(V_1 - V)]^3} ,$$

and

$$\frac{dG}{dV} = \frac{(2 + \Gamma) \Gamma (V_1 - V_2)}{[2V - \Gamma(V_2 - V)]^2} .$$

Solving,

$$\dot{V} = 2U_s \dot{U}_p / \left(V_2 \frac{dP}{dV} - U_s^2 \rho_2 \right)$$

and then

$$\dot{P} = \frac{dP}{dV} \dot{V} .$$

Assume $P_m \equiv 0$, if pressure gradient is not known.

Calculate

$$P_\tau = \dot{P} - \rho_0 U_s P_m$$

$$V_\tau = (\dot{U}_p + P_m) / (\rho_0 U_s)$$

$$I_\tau = -PV_\tau .$$

Solve for W ,

$$P = H(V, I, W) .$$

(The HOM equation of state is a Grüneisen construction.)

Solve for W_τ ,

$$P_\tau = H_V V_\tau + H_I I_\tau + H_W W_\tau .$$

V. FFIRE

This solution method forms the basis for the computer program FFIRE (LASL Identification No. LP-0601). Two examples of the output from the program follow. The first example is the calculation of the decomposition rate for PBX 9404 at density 1.844. The second example is the calculation of the rate and POP-PLOT for PBX 9404 at density 1.72 using the data at density 1.844. A microfiche listing the code is in the pocket on the inside back cover of this report.

Notation for computer program FFIRE.

RUN = distance to detonation (cm)

P = pressure (Mbar)

V = specific volume (cm³/g)

UP = shock particle velocity (cm/μs)

US = shock velocity (cm/μs)

W = mass fraction of undecomposed explosive

RATE = $-\frac{dW}{dt} \cdot \frac{1}{W}$, decomposition rate (μs^{-1})

TEMPERATURE = (K)

TIME = time to detonation (μs)

RHO = density (g/cm^3)

EXAMPLE 1

```
9424 B      PBX9404,BEST (TDET,UP,RUN) POP PLOT (.020,1.70) TO (.200,0.05) 7MAR78  RH0 = 1,84400
POP PLOT, LN(RUN) = A1 + A2*LN(P=A3), A1 = -5.460553E+00 A2 = -1.531479E+00 A3 = -0.
REACTION HUGONIOT, US = C + S*UP,      C = 2.460000E+01 S = 2.530000E+00
CJ DETONATION VELOCITY = 8.880000E-01

HOM EQUATION OF STATE CONSTANTS
PBX9404, RH0=1.844, RAMSAY INERT HUGONIOT
UNREACTED EXPLOSIVE
2.4230000000E-01 1.88300000000E+00 1.0000000000E-02=0,
-0.          -9.04187222042E+00-7.13185252435E+01-1.25204979360E+02
-9.20424177603E+01-2.21893826727E+01 6.75000000000E-01 4.00000000000E-01
5.42299349241E-01 5.00000000000E-05 0.          -0,
3.00000000000E+02 1.000000000200E+06=0.          -0,
-0.          -0.          -0.
DETONATION PRODUCTS
-3.53906259964E+00-2.57737590393E+00 2.60075423332E-01 1.39083578508E-02
-1.13963024075E+02-1.61913041133E+00 5.21518534192E-01 6.77506594107E+02
4.26524264691E+03 1.04679999902E+04 7.36422919790E+00-4.93658222389E+01
2.92353060961E+02 3.30277402219E+02-1.14532498206E-02 5.00000000000E+01
1.00000000000E+01
```

EXAMPLE 1 (cont)

9404 B PBX9404, REST (TDET, UP, RUN) POP PLOT (.020, 1.74) TO (.200, 0.05) 7MAR78 RHO = 1.844MM
 POP PLOT, LN(RUN) = A1 + A2*LN(P=A3), A1 = -5.460553E+00 A2 = -1.551479E+00 A3 = -0,
 REACTION HUGONIOT, US = C + S*UP, C = 2.460000E-01 S = 2.530000E+00

RUN	P	V	UP	US	W	RATE	TEMPERATURE	TIME
6,49135	.00700	.51609	.01354	.28027	.99788	9.9065E-04	320,74243	.27,42226
6,92189	.00800	.51325	.01525	.28457	.99734	1.4325E-03	324,34745	.21,86340
5,78018	.00900	.51056	.01690	.28877	.99676	1.9314E-03	328,05044	.17,87969
4,91955	.01000	.50801	.01852	.29285	.99613	2.5920E-03	331,85493	.14,91958
1,69451	.02000	.48807	.03293	.32933	.98813	1.7859E-02	375,04071	.4,41910
.90723	.03000	.47432	.04516	.36026	.97800	5.5259E-02	425,34669	.2,12173
.58149	.04000	.46399	.05597	.38759	.96657	1.2383E-01	480,03671	.1,24737
.41121	.05000	.45582	.06576	.41236	.95422	2.3291E-01	537,35231	.82060
.30939	.06000	.44912	.07477	.43517	.94118	3.9244E-01	596,25659	.57990
.24293	.07000	.44348	.08317	.45642	.92756	6.1326E-01	656,08883	.43061
.19677	.08000	.43863	.09107	.47640	.91343	9.0730E-01	716,45485	.33153
.16319	.09000	.43441	.09854	.49530	.89882	1.2877E+00	777,02884	.26236
.13788	.10000	.43068	.10565	.51329	.88378	1.7699E+00	837,67799	.21213
.11825	.11000	.42735	.11245	.53049	.86829	2.5704E+00	898,27342	.17450
.10267	.12000	.42435	.11897	.54699	.85236	3.1087E+00	958,72521	.14555
.09006	.13000	.42163	.12525	.56288	.83597	4.0066E+00	1018,98553	.12282
.07968	.14000	.41915	.13131	.57821	.81911	5.1307E+00	1079,01508	.10462
.07102	.15000	.41687	.13717	.59304	.80179	6.3859E+00	1138,73142	.98983
.06371	.16000	.41476	.14285	.60741	.78396	7.9333E+00	1198,15217	.97765
.05747	.17000	.41281	.14837	.62157	.76560	9.7694E+00	1257,25020	.96749
.05210	.18000	.41100	.15373	.63495	.74668	1.1942E+01	1316,00279	.95893
.04743	.19000	.40930	.15896	.64818	.72718	1.4486E+01	1374,38483	.95165
.04334	.20000	.40771	.16406	.66108	.70706	1.7551E+01	1432,37493	.94541
.03974	.21000	.40622	.16904	.67369	.68625	2.1107E+01	1489,98234	.94001
.03655	.22000	.40482	.17391	.68601	.66475	2.5308E+01	1547,16312	.93532
.03371	.23000	.40349	.17868	.69806	.64250	3.0261E+01	1603,88563	.93121
.03116	.24000	.40223	.18335	.70987	.61946	3.6140E+01	1660,13228	.92759
.02887	.25000	.40104	.18792	.72144	.59554	4.3198E+01	1715,90459	.92439
.02680	.26000	.39991	.19241	.73280	.57076	5.1403E+01	1771,10946	.92154
.02492	.27000	.39883	.19682	.74395	.54498	6.1327E+01	1825,77546	.91899
.02321	.28000	.39780	.20114	.75490	.51817	7.3252E+01	1879,84537	.91671
.02165	.29000	.39682	.20540	.76566	.49021	8.7814E+01	1933,34237	.91466
.02022	.30000	.39588	.20958	.77625	.46105	1.0559E+02	1986,08317	.91280
.01890	.31000	.39498	.21370	.78667	.43060	1.2763E+02	2058,15329	.91111
.01769	.32000	.39412	.21776	.79693	.39875	1.5534E+02	2089,46643	.90958
.01657	.33000	.39329	.22175	.80703	.36537	1.9085E+02	2139,97351	.90818
.01553	.34000	.39249	.22569	.81699	.33038	2.3707E+02	2189,60412	.90691
.01457	.35000	.39173	.22956	.82680	.29360	2.9954E+02	2258,31627	.90573
.01367	.36000	.39099	.23339	.83648	.25488	3.8714E+02	2286,03733	.90466
.01283	.37000	.39028	.23717	.84603	.21405	5.1701E+02	2332,69611	.90366
.01205	.38000	.38959	.24089	.85546	.17090	7.2638E+02	2378,21644	.90215
.01132	.39000	.38893	.24457	.86477	.12528	1.1093E+03	2422,49717	.90190
.01064	.40000	.38829	.24820	.87396	.07686	2.0266E+03	2465,46237	.90111
.01000	.41000	.38767	.25179	.88304	.03000	5.7971E+03	2506,29194	.90038

EXAMPLE 2

```
9404 8      PBX9404,BEST (TDET,UP,RUN) POP PLOT (.020,1.70) TO (.200,0,05) 7MAR78  RHO = 1.72000
POP PLOT, LN(RUN) = A1 + A2*LN(P=A3), A1 = -5.460553E+00 A2 = -1.531479E+00 A3 = -0,
REACTION HUGONIOT, US = C + S*UP,      C = 2.460000E-01 S = 2.530000E+00
CJ DETONATION VELOCITY = 8.880000E-01

HOM EQUATION OF STATE CONSTANTS
PBX9404, RHO=1.844, RAMSAY INERT HUGONIOT
UNREACTED EXPLOSIVE
2.4230000000E-01 1.8830000000E+00 1.0000000000E-02=0,
-0,      -9.04187222042E+00-7.13186252435E+01-1.25204979360E+02
-9.20424177603E+01-2.21893825727E+01 6.7500000000E-01 4.0000000000E-01
5.42299349241E-01 5.0000000000E-05 0,      -0,
3.0000000000E+02 1.0000000000E-06=0,      -0,
-0,      -0,
DETONATION PRODUCTS
-3.53906259964E+00-2.57737590393E+00 2.60075423332E-01 1.39083578508E-02
-1.13963024075E-02-1.61913041133E+00 5.21518534192E-01 6.77506594107E-02
4.26524264691E-03 1.04679999902E+04 7.36422919790E+00-4.93658222389E-01
2.92353060961E-02 3.30277402219E-02-1.14532498206E-02 5.00000000000E-01
1.00000000000E-01
```

EXAMPLE 2 (cont)

9404 B PBX9404,BEST (TDET,UP,RUN) PUP PLOT (.020,1,70) TO (.200,0,05) 7MAR78 RHO = 1.72000
 POP PLUT, LN(RUN) = A1 + A2*LN(P=A3), A1 = -5.460553E+00 A2 = -1.531479E+00 A3 = 0.
 REACTION HUGONIOT, US = C + S*UP, C = 2.460000E-01 S = 2.530000E+00

RUN	P	V	UP	US	N	RATE	TEMPERATURE	TIME
8,43730	.00200	.53358	.00978	.11890	.99800	4.5703E-04	314,26523	50,15897
6,12251	.00300	.52971	.01245	.14007	.99800	8.7965E-04	317,25236	32,13292
4,76500	.00400	.52611	.01487	.15638	.99800	1.4504E-03	320,12791	22,93681
3,86836	.00500	.52275	.01712	.16975	.99800	2.1950E-03	322,91333	17,42482
3,23232	.00600	.51959	.01926	.18115	.99800	3.1192E-03	325,62936	13,79385
2,75878	.00700	.51663	.02129	.19113	.99796	4.2422E-03	328,44922	11,24694
2,39354	.00800	.51383	.02325	.20006	.99744	5.6137E-03	333,15050	9,37804
2,10405	.00900	.51118	.02514	.20815	.99688	7.0357E-03	337,94663	7,95872
1,86958	.01000	.50867	.02697	.21559	.99628	8.8851E-03	342,84125	6,85147
.81030	.02000	.48898	.04299	.27047	.98858	4.4669E-02	396,78844	2,38729
.47582	.03000	.47536	.05640	.30925	.97882	1,2194E-01	457,70456	1,22302
.32096	.04000	.46510	.06820	.34098	.96779	2.5507E-01	522,95200	.74439
.23454	.05000	.45697	.07887	.36856	.95588	4.5897E-01	590,81475	.50005
.18058	.06000	.45030	.08869	.39332	.94329	7.4960E-01	660,26478	.35808
.14423	.07000	.44467	.09783	.41600	.93013	1.1442E+00	730,64455	.26811
.11838	.08000	.43983	.10642	.43706	.91648	1.6620E+00	801,53295	.20742
.09922	.09000	.43501	.11455	.45681	.90237	2.3236E+00	872,65926	.16451
.08455	.10000	.43188	.12228	.47547	.88784	3.1536E+00	943,81556	.13302
.07304	.11000	.42855	.12967	.49321	.87288	4.1782E+00	1014,889/1	.10923
.06379	.12000	.42554	.13676	.51016	.85749	5.4276E+00	1085,78323	.09019
.05624	.13000	.42282	.14358	.52641	.84167	6.9363E+00	1156,44049	.07622
.04998	.14000	.42033	.15016	.54204	.82540	8.7458E+00	1226,79398	.06449
.04472	.15000	.41804	.15653	.55713	.80867	1.0842E+01	1296,82357	.05492
.04025	.16000	.41593	.16271	.57172	.79147	1.3443E+01	1300,46674	.04649
.03641	.17000	.41398	.16870	.58586	.77376	1.6452E+01	1435,71918	.04036
.03309	.18000	.41215	.17454	.59959	.75553	1.9991E+01	1504,55269	.03476
.03019	.19000	.41045	.18022	.61295	.73671	2.4425E+01	1572,96302	.02997
.02765	.20000	.40886	.18576	.62596	.71735	2.8994E+01	1640,84972	.02586
.02539	.21000	.40736	.19118	.63864	.69733	3.4735E+01	1708,27782	.02230
.02339	.22000	.40594	.19647	.65104	.67664	4.1436E+01	1775,19704	.01919
.02160	.23000	.40461	.20164	.66315	.65524	4.9275E+01	1841,56548	.01646
.01999	.24000	.40335	.20672	.67501	.63310	5.8489E+01	1907,35210	.01405
.01854	.25000	.40215	.21169	.68662	.61015	6.9406E+01	1972,53736	.01192
.01722	.26000	.40101	.21657	.69800	.58634	8.2231E+01	2037,08237	.01062
.01602	.27000	.39992	.22135	.70917	.56162	9.7493E+01	2100,95551	.00832
.01493	.28000	.39889	.22606	.72013	.53591	1.1570E+02	2164,11473	.00679
.01393	.29000	.39790	.23068	.73090	.50916	1.3752E+02	2226,51479	.00541
.01302	.30000	.39695	.23523	.74148	.48125	1.6416E+02	2288,13165	.00416
.01217	.31000	.39685	.23970	.75190	.45214	1.9663E+02	2348,88985	.00303
.01139	.32000	.39518	.24411	.76214	.42171	2.3685E+02	2408,74563	.00200
.01067	.33000	.39434	.24845	.77223	.38987	2.8746E+02	2467,64144	.00106
.01000	.34000	.39354	.25273	.78217	.35649	3.5241E+02	2525,51567	.00020

REFERENCES

1. C. L. Mader and C. A. Forest, "Two-Dimensional Homogeneous and Heterogeneous Detonation Wave Propagation," Los Alamos Scientific Laboratory report LA-6259 (June 1976).
2. C. L. Mader and M. S. Shaw, "Users Manual for SIN: A One-Dimensional Hydrodynamic Code for Problems Which Include Chemical Reactions, Elastic-Plastic Flow, Spalling, Phase Transitions, Melting, FOREST FIRE, Detonation Build-up, and SESAME Tabular Equation of State," Los Alamos Scientific Laboratory report LA-7264-M (1978).
3. J. B. Ramsey and A. Popolato, "Analysis of Shock Wave and Initiation Data for Solid Explosives," Fourth Intern. Symposium on Detonation, White Oak, MD, October 1965, ACR-126 (1965), p. 233.
4. R. G. McQueen, S. P. Marsh, J. W. Taylor, and J. N. Fritz, Chap. VII of High Velocity Impact Phenomena, R. Kinslow, Ed. (Academic Press, 1970).
5. B. G. Craig, Los Alamos Scientific Laboratory, unpublished wedge test data.
6. J. D. Wackerle, Los Alamos Scientific Laboratory, unpublished wedge test data.
7. D. Stirpe, J. O. Johnson, and J. D. Wackerle, "Shock Initiation of XTX-8003 and Pressed PETN," J. Appl. Phys. 41, 3884 (1970).
8. G. E. Seay and L. B. Seely, Jr., "Initiation of a Low-Density PETN Pressing," J. Appl. Phys. 32, 1092 (1961).